DALTON
PERSPECTIVE

The rational design of high symmetry coordination clusters†

Dana L. Caulder and Kenneth N. Raymond *

Department of Chemistry, University of California, Berkeley, CA 94720-1460, USA. E-mail: raymond@socrates.berkeley.edu

Received 28th October 1998, Accepted 10th December 1998

There are numerous examples of supramolecular assemblies based on metal–ligand interactions. Many have been synthesized unintentionally, while others have been the result of systematic variation of metal and ligand components. Until recently, no one has provided a rational synthetic methodology for the synthesis of metal–ligand coordination clusters. We have provided a model for the assembly of naturally-occurring, high-symmetry protein assemblies such as ferritin (*O* symmetry) and viral protein coats (*I* symmetry) based on incommensurate symmetry interactions. This model has led us to develop a rational synthetic approach to the synthesis of high-symmetry clusters based on the metal–ligand coordinate bond. Herein we describe our design strategies, provide examples of triple helicates of stoichiometry M_2L_3 and tetrahedral clusters of stoichiometry M_4L_6 and M_4L_4, and discuss the solution dynamics of these clusters.

High symmetry clusters in nature

Supramolecular chemistry, which has been called a molecular information science, describes the spontaneous assembly of non-covalently linked molecular clusters of unique shape and composition.[1] This requires both a driving force and a dynamic system so that all possible molecular structures can be explored to generate the formation of the thermodynamically favored, ideally pre-designed, assembly. An example of such a structure in nature is the iron storage protein apoferritin (Fig. 1).[2,3] The protein is composed of 24 non-covalently linked protein subunits that form a nearly spherical shell of octahedral symmetry. Inside the shell up to 4,500 iron atoms can be stored in the form FeO(OH). In effect, ferritin operates to keep iron in solution as a small particle of rust by stopping the growth of the iron oxide particle before it reaches a size that would result in precipitation. Remarkably, when the apoprotein is dissociated into the individual subunits and allowed to reassemble, only the highly symmetric 24 subunit cluster forms.[4] Intermediate assemblies of less than the full 24 complement are only transiently stable.

Similar structures are seen in many viruses, in which non-covalently linked assemblies of protein subunits are used to protect the viral nucleic acid. Again, it is generally true that dissociation and reassembly of the protein coat does not give a random polymeric assembly, but instead only the highly symmetric cluster, in many cases 60-mers with icosahedral symmetry.[5,6] Viral coats of this stoichiometry and the ferritin cluster correspond to the pure rotation groups *I* and *O*, with 60 and 24 symmetry elements, respectively. That is, each of the protein subunits in the examples given constitutes an asymmetric unit of the cluster.‡

† This review covers papers in our series Coordination Number Incommensurate Cluster Formation. For the most recent paper in that series see ref. 82.

‡ In the case of certain viruses, a four protein bundle makes up one of the 60 subunits.[7]

Kenneth N. Raymond was born on January 7, 1942 in Astoria, Oregon. He obtained a B.A. from Reed College in 1964 and Ph.D. in 1968 from Northwestern University (with Basolo and Ibers). He was appointed Assistant Professor at the University of California, Berkeley on July 1, 1967, becoming Associate Professor in 1974 and Professor in 1978. He has served as Vice Chair for the Berkeley Chemistry Department (1982–1984) and Chair (1993–1996). He was Chair of the ACS Division of Inorganic Chemistry in 1996. He received the Lawrence Award of the Department of Energy in 1984, a Humboldt Research Award in 1992, the ACS Bader Award in Bioinorganic Chemistry in 1994 and was elected to the National Academy of Sciences in 1997. He has a long-standing interest in coordination chemistry, both synthetic and biological.

Kenneth N. Raymond

Dana L. Caulder was born in Columbia, South Carolina in 1972. She earned her B.S. in chemistry from the University of South Carolina in 1994 and Ph.D. from the University of California, Berkeley in 1998. Her Ph.D. thesis focused on the rational design of high symmetry coordination clusters and the investigation of the unique kinetic and thermodynamic properties of these clusters. Currently she is dividing her time between UCB and the Lawrence Berkeley National Laboratory. At UCB she is the assistant crystallographer and at LBNL she is investigating actinides by XAFS techniques.

Dana L. Caulder

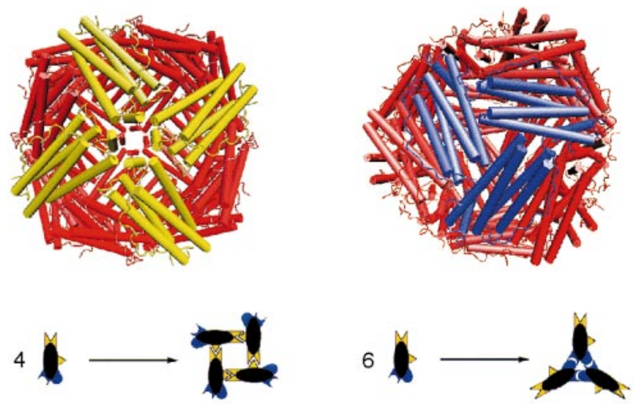

Fig. 1 Based on the crystal structure of human H chain ferritin,[8] the octahedral 24-subunit iron storage protein as viewed down the four-fold (left) and three-fold (right) axes. The four helix bundle protein subunits that directly interact at these symmetry axes are highlighted in yellow and blue, respectively. The interaction at the four-fold axis, in which the lock and key are 90° apart, requires the formation of tetramers. Similarly, the interaction at the three-fold axis, in which the lock and key are 60° apart, requires the formation of trimers.

Consider again the octahedral symmetry ferritin cluster. Interaction of the protein subunits at the four-fold axis (the view direction in Fig. 1) can be considered a lock-and-key interaction in which the lock and key are 90° apart (Fig. 1). The interaction around the four-fold axis is both a symmetry and stoichiometry requirement: it requires formation of tetramers from the monomeric subunit. Similarly, the interaction of the protein subunits at the three-fold axis (the view direction in Fig. 1, top right) can be regarded as a lock-and-key interaction in which the lock and key are positioned 60° apart (Fig. 1, bottom right). The result is a stoichiometry requirement to form trimers. *Simultaneous satisfaction of these two incommensurate n-fold symmetry axes can only be satisfied by formation of a cluster with octahedral symmetry.* In a similar fashion the icosahedral cluster is formed through the combination of incommensurate lock-and-key interactions with five-fold and three-fold symmetry.

The term "incommensurate" is used in the same sense as applied to incommensurate lattices. When a planar crystal layer with one lattice spacing is deposited on a structurally similar layer with a slightly different lattice spacing, the two layers must curve in order for the unit cells to remain in registry. This is what drives the formation of some naturally-occurring tubular structures.[9] In the case of a discrete closed cluster such as ferritin, the surface lattice must curve to satisfy the two incommensurate symmetry interactions. The information for this curvature is programmed into the subunits as the angle between the three-fold and four-fold axes.

Rational design of high symmetry coordination clusters

The protein–protein interactions described above are formed from many weak hydrogen bonding and van der Waals contacts along large regions or surfaces. The complicated sum of these many individual interactions can still be described by a single vectorial relationship that represents the geometry of the highly directional lock-and-key interactions described above. Metal–ligand interactions, on the other hand, are strong and highly directional, and can be used in place of many weak interactions to direct the formation of multi-metal coordination clusters.

There are examples of one-, two- and three-dimensional polymeric assemblies using metals and ligands.[10–16] There are also numerous discrete structures, including helices, tetrahedra, squares and cubes among others.[17–50] Most of these interesting complexes have been discovered fortuitously by systematic variation of ligand and metal components. Only recently has there been progress towards developing a *rational* synthetic approach to the design and synthesis of such architectures.[17–19,21,25,36,38–40,48,51–53]

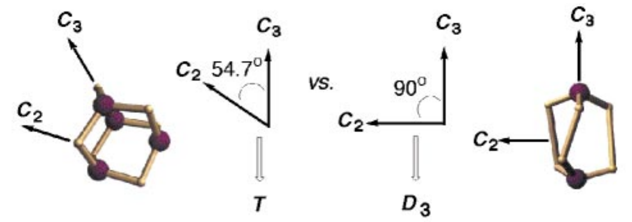

Fig. 2 The orientation of the C_3 and C_2 symmetry axes determines whether a T symmetry tetrahedron or a D_3 symmetry triple helix will form.

In principle, the formation of clusters of any symmetry should be possible. To do so, the symmetry elements of a particular point group need to be considered. In order to design a cluster with D_3 symmetry, an M_2L_3 triple helicate[41] for example, both the C_2 and C_3 axes of the point group must be taken into account. A C_2-symmetric bis(bidentate) ligand can provide the 2-fold axis, while a metal ion with pseudo-octahedral coordination by three bidentate chelators can provide the 3-fold axis. These symmetry axes *must*, however, be oriented 90° to one another (Fig. 2). A cluster with T symmetry, an M_4L_6 tetrahedron[17,27,37,50,54] for example, is also possible with the same combination of symmetry elements. In this type of cluster, however, the C_2 and C_3 axes must be oriented 54.7° from one another (Fig. 2).

Design strategies

The metal coordination geometry and the orientation of the interaction sites in a given ligand provide the instructions, or blueprint, for the self-assembly of the proposed cluster. As a result, there are several important considerations in designing these supramolecular assemblies based on metal–ligand interactions. Firstly, we choose to use multi-branched *chelating* ligands because of their increased preorganization and stronger binding as a result of the chelate effect;[55] although, there are numerous examples of supramolecular assemblies based upon multibranched monodentate ligands.[25,26,36,40] Secondly, the orientation of the multiple binding units within a ligand must be rigidly fixed so that other, unwanted, cluster stoichiometries or geometries are avoided. Thirdly, because the self-assembly of the thermodynamically-favored cluster from the ligand and metal components involves the making of many metal–ligand bonds, the metals should be labile so that "mistakes" resulting from the initial formation of kinetic products can be corrected.

Catecholamide and hydroxamate ligands are excellent choices for binding units in supramolecular complexes because of the high stability and lability of these chelates with +3 metal ions with octahedral coordination environments.[56–61] Recently, hydroxypyridinone[62] (HOPO) and pyrazolone[63] ligands have also proven useful in synthesizing supramolecular clusters (Fig. 3). Three catecholamide units coordinating a +3 metal ion will generate a −3 charge for the $M(catam)_3$ unit. In contrast, the hydroxamates, hydroxypyridinones and pyrazolones will form neutral $M(ligand)_3$ units.

As part of our approach, the feasibility of the proposed metal–ligand system is explored prior to ligand synthesis using molecular mechanics calculations.[64] Although these calculations do not guarantee that the proposed structure will form, they do help eliminate unsuitable structures. If the metal coordination and ligand geometry are correctly chosen, the intended supramolecular cluster should be the only structure that satisfies the binding requirements of the metal, while not creating unfavorable steric interactions in the ligands.

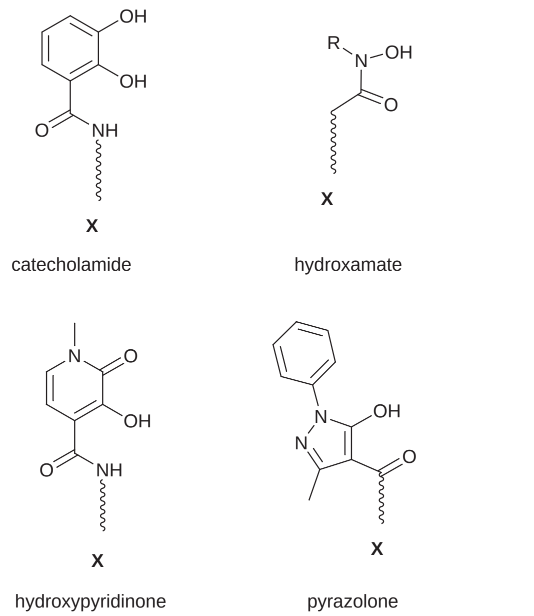

Fig. 3 Catecholamides, hydroxamates, hydroxypyridinones and pyrazolones are useful chelating units for synthesizing supramolecular clusters because of their high stability and lability with +3 metal ions such as Al(III), Ga(III) and Fe(III).

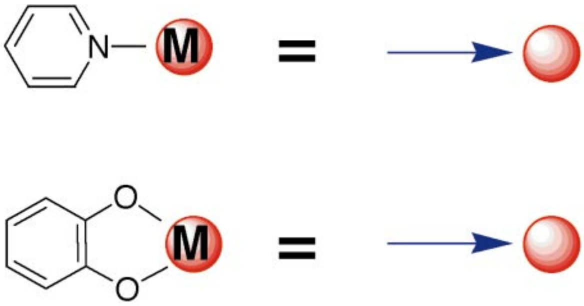

Fig. 4 In the case of a monodentate ligand, the **Coordinate Vector** is the vector from the coordinating atom of the ligand directed towards the metal center. In the case of a bidentate ligand, the coordinate vector is the vector that bisects the chelating group and is directed toward the metal ion.

Definitions

In order to describe this approach to rational design, it will be useful to define terms that more accurately describe the relevant geometric relationships. The vector that represents the interaction between a ligand and metal is the **Coordinate Vector** (Fig. 4).§ In the case of a monodentate ligand, this vector is simply the one directed from the coordinating atom of the ligand towards the metal ion. In the case of a bidentate ligand, this vector bisects the bidentate chelating group and is directed towards the metal ion.

When using chelating ligands, the plane orthogonal to the major symmetry axis of a metal complex is the **Chelate Plane** (Fig. 5); all of the coordinate vectors of the chelating ligands lie in the chelate plane. Any symmetric coordination complex cluster can be described in terms of the relationships between these chelate planes. In principle, by careful pre-arrangement of coordinate vectors in a multibranched ligand, programming of a cluster of any symmetry or stoichiometry becomes feasible.

Although the twist angle[55] is a common measure of the

§ Although we previously used the term *chelate* vector to describe the interaction between a bidentate ligand and a metal ion, we now use the term *coordinate* vector so that the term is more general and applicable to describing the numerous supramolecular systems based on monodentate ligands.

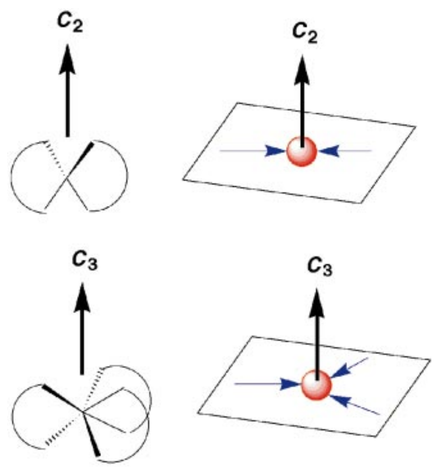

Fig. 5 The plane orthogonal to the major symmetry axis of the metal complex is the **Chelate Plane**. In the case of bidentate chelators, all of the coordinate vectors lie in the chelate plane.

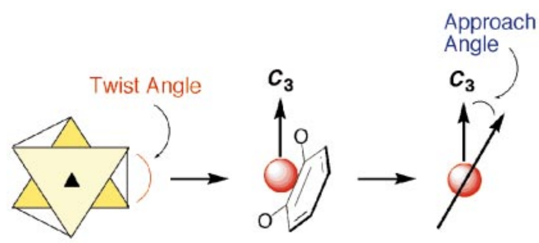

Fig. 6 An alternative measure of the arrangement of three bidentate chelators around a metal ion is the **Approach Angle**, which is the angle between the vector connecting the two coordinating atoms of a bidentate ligand projected down the (pseudo) 2-fold axis of the chelate group and the major symmetry axis of the metal center.

arrangement of three bidentate chelators around a metal ion,¶ the **Approach Angle** has the advantage that it provides a measure that can be readily compared to angles generated by a given high symmetry cluster (Fig. 6). The approach angle is the angle between the vector connecting the two coordinating atoms of a bidentate ligand projected down the (pseudo) 2-fold axis of the chelate group and the major symmetry axis of the metal center. A twist angle of 60° corresponds to an approach angle of 35.3°, while a twist angle of 0° corresponds to an approach angle of 0°.

M_2L_3 Complexes

Triple helicates

The simplest multi-metal cluster contains two metal sites linked by one or more ligands. When these two metal ions are linked by three identical, C_2-symmetric ligand strands the resulting bimetallic cluster is called a triple helicate if both metal ions have the same chirality. This chiral M_2L_3 complex has idealized D_3 symmetry: the C_3 axis is coincident with, and the three C_2 axes are perpendicular to, the helical axis of the complex. There are numerous examples of clusters of this type (Fig. 7).[19,45,65–69] An early example of a triple helicate is the iron(III) complex of the dihydroxamate siderophore rhodotorulic acid (H_2**11**), which is produced by the yeast *Rhodotorula mucilaginosa* (previously *R. piliminae*).[70,71] Rhodotorulic acid enantioselectively forms a Δ-*cis* complex of Fe_2**11**$_3$ stoichiometry at neutral pH, and this complex is currently the only known naturally-occurring example of a triple helicate (Fig. 8). Later, the Fe(III) complex of a hydroxypyridinone (H_2**12**) analogue of rhodotorulic acid

¶ A twist angle of 60° corresponds to that of a perfect octahedral metal complex, while a twist angle of 0° corresponds to that of a trigonal prismatic metal complex.

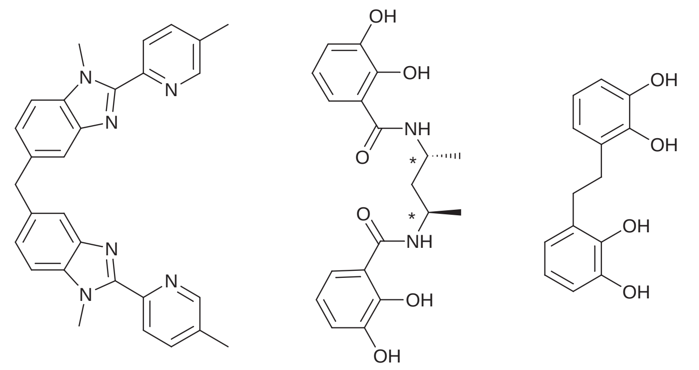

1 H_4**2** H_4**3**

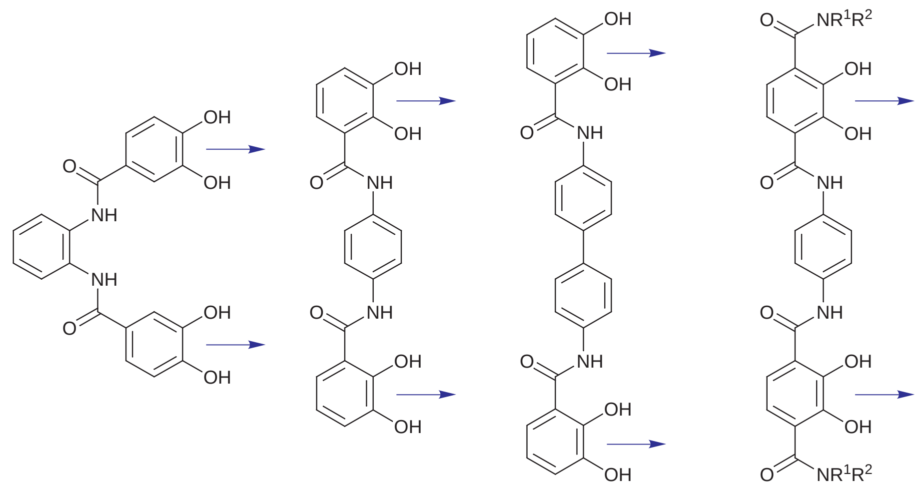

H_4**4** H_4**5** H_4**6**

H_4**7**	$R^1=R^2=H$
H_4**8**	$R^1=R^2=Pr^i$
H_4**9**	$R^1=Pr^i$, $R^2=Me$
H_4**10**	$R^1=R^2=(S)\text{-CHMePh}$

Fig. 7 Ligands which form M_2L_3 triple helicates. Ligands **1**,[68] H_4**2**[45] and H_4**3**[67] form helicates with Co(III), Ga(III) and Ti(IV), respectively. Ligands H_4**4**–H_4**10** were designed to make M_2L_3 triple helicates with +3 metal ions like Ga(III), Al(III) and Fe(III).[19,65,66] The arrows represent the coordinate vectors, which should be parallel (or be able to become parallel upon complexation), pointing in the same direction if a triple helicate is to form.

was structurally characterized (Fig. 8); the crystalline Λ,Λ-Fe_2**12**$_3$ complex encapsulates a molecule of water.[72]

As mentioned above, in order to *rationally design* an M_2L_3 triple helicate with idealized D_3 symmetry, both C_2 and C_3 axes must be encoded. Using a metal ion with pseudo-octahedral coordination and a C_2 symmetric bis(bidentate) ligand, these symmetry axes can be generated (*vide supra*). These symmetry axes *must*, however, be oriented 90° to one another. Because the two metal centers share the same C_3 helical axis, the two *chelate planes* in a triple helix must be parallel (Fig. 9). Although a flexible linker may *allow* for the formation of an M_2L_3 triple helicate, a rigid linker can *direct* the formation of an M_2L_3 triple helicate.

Based on this design strategy, a series of M_2L_3 triple helicates based on ideally planar bis(bidentate) catecholamide ligands has been synthesized (H_4**4**–H_4**10**, Fig. 7).[19,65,66] The rigid aromatic linkers serve to maintain preorganization of the ligand, since other topologies are possible when flexible linkers are used (*vide infra*).‖ The chelate vectors, indicated as arrows, are parallel and point in the same direction within each ligand. Molecular mechanics calculations indicated that for each of these ligands the chiral helicate was lower in energy than the *meso*-M_2L_3 cluster.[64] The M_2L_3 stoichiometry was confirmed by both fast atom bombardment (FAB) and electrospray mass spectrometry. The crystal structure of the Ga(III) complex of H_4**5** is shown in Fig. 10 and confirms that the rigid ligand forms a racemic mixture of homochiral triple helicates with Ga(III).

Triple mesocates

A *non-chiral* M_2L_3 cluster has a Δ-configuration at one and a Λ-configuration at the other metal center, and, therefore, will be called a *meso*-complex or a mesocate.** This type of cluster has idealized C_{3h} symmetry: rather than having three C_2 axes perpendicular to the C_3 axis, there is an orthogonal mirror plane that relates the Δ- to the Λ-configured metal center. What factors control the formation of a mesocate *versus* a helicate? Although it has been proposed that the length of an alkyl spacer between two chelating moieties may direct helicate *versus* mesocate formation[73,76] or that a chiral ligand may be able to

‖ Note, however, that a rigid backbone is not necessary if the linker is short enough to prevent both ends of the ligand from coordinating a single metal.[45,67]

** Since a helix by definition is chiral, the term *meso-helicate*[73–75] is an oxymoron and will not be used.

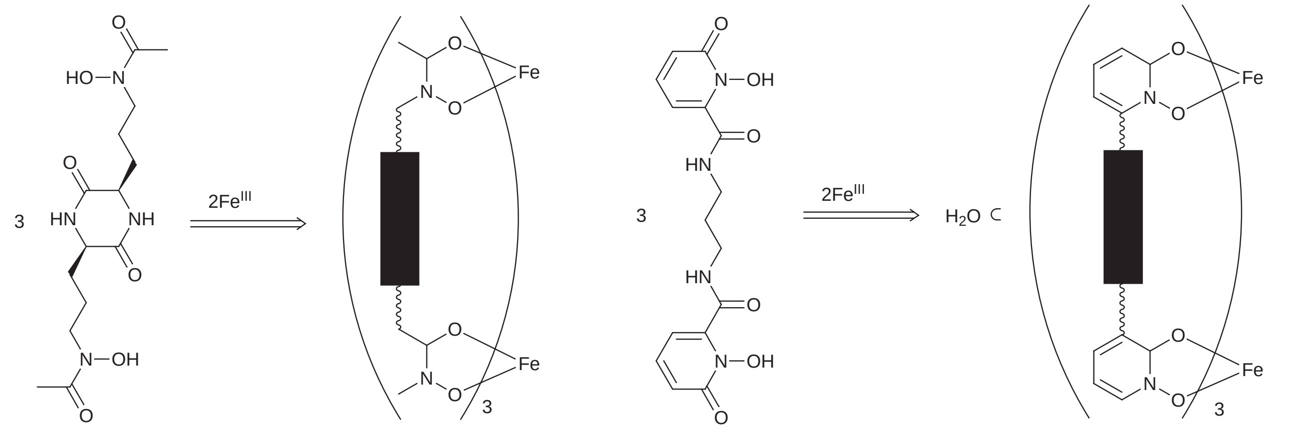

H_2**11** Fe_2**11**$_3$ H_2**12** $H_2O \subset Fe_2$**12**$_3$

Fig. 8 The dihydroxamate siderophore rhodotorulic acid forms an enantiomerically pure Δ,Δ-triple helicate with Fe(III).[70,71] The bis(hydroxypyridinone) ligand H_2**12** was synthesized as a rhodotorulic acid analogue and forms a *rac*-(ΔΔ/ΛΛ) Fe_2**12**$_3$ triple helicate encapsulating a molecule of H_2O.[72]

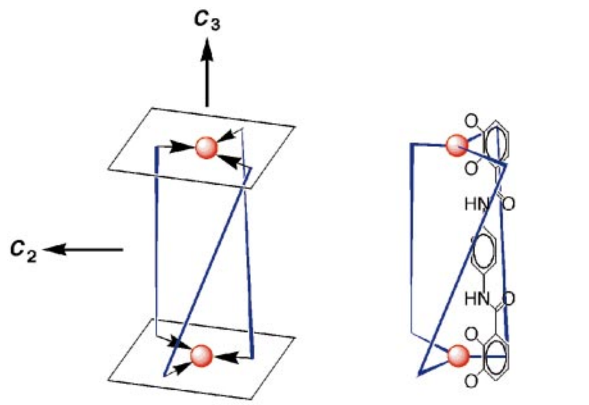

Fig. 9 In a D_3 symmetric triple helicate, the chelate planes are parallel. The spheres represent the pseudo-octahedral metal ions, the rods represent the ligands, and the arrows on the ligand rods indicate the coordinate vectors.

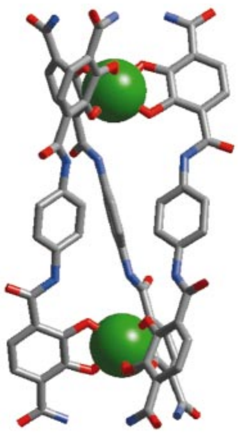

$[Ga_2 7_3]^{6-}$

Fig. 10 The crystal structure of the triple helicate $[Ga_2 7_3]^{6-}$.

induce a helical twist in an M_2L_3 complex these explanations do not seem convincing.[45]

Recently we have presented the first example of a ligand (H_2**13**) that makes *both* a helicate and a mesocate.[77] Remarkably, the X-ray analysis showed that in the solid state the Al_2**13**$_3$ complex is a chiral helicate (racemic), while the Ga_2**13**$_3$ complex is an achiral mesocate (Fig. 11). Although both complexes contain the same ligand, the structures are markedly different: the distance between the two metal centers in Al_2**13**$_3$ is 7.13 Å, while in Ga_2**13**$_3$ this distance is 9.74 Å. The structures show that the helical cavity of Al_2**13**$_3$ contains one encapsulated water molecule, while no encapsulated solvent was found in the Ga_2**13**$_3$ mesocate (Fig. 11). The encapsulated water molecule in Al_2**13**$_3$ is in close contact (2.9–3.0 Å) with six phenolic oxygen atoms that are pointing into the helicate cavity. The rather polar cavity of Al_2**13**$_3$ forces the six hydrophobic methyl groups of the aliphatic linkers to point outwards. Only three methyl groups in Ga_2**13**$_3$ are pointing outwards, while the remaining three methyl groups are directed into the cluster interior and are shielded from interaction with the solvent (Fig. 11).

Other topologies

Other topologies are also possible for M_2L_3 clusters. For example, the dihydroxamate siderophore alcaligin forms an M_2L_3 complex with Fe(III) in which each metal center is coordinated by one tetradentate and one bridging bis(bidentate) alcaligin ligand (H_2**14**, Fig. 12).[78] A similar structure type has recently been reported by McCleverty and coworkers (**15**, Fig. 12).[27] The alcaligin topology is more likely with the use of flexible ligands that can wrap around and coordinate a single metal ion, thus the use of *rigid* linkers can be used to avoid this topology.

M_4L_6 Complexes

Another cluster with the same ligand to metal ratio as the M_2L_3 triple helicate is the M_4L_6 tetrahedron, where the four metal ions act as the vertices and the six ligands act as the edges of the tetrahedron. Depending on the chiralities at the metal centers, the cluster can have either idealized C_3 (ΔΛΛΛ/ΛΔΔΔ), S_4 (ΔΔΛΛ) or T (ΛΛΛΛ/ΔΔΔΔ) symmetry. The first examples of M_4L_6 tetrahedral clusters were the surprises that Saalfrank and coworkers characterized as adamantoid-type clusters of both S_4 and T symmetry (H_2**16** and H_2**17**, Figs. 13 and 14).[50,54,79] Remarkably, an ammonium cation was found to be encapsulated by one of these tetrahedral clusters.[50]

We have demonstrated the utility of the incommensurate symmetry interaction model in two approaches to the *rational design* of such clusters. Both approaches employ an ideally planar C_2-symmetric bis(bidentate) ligand with a rigid backbone, but the orientation of the C_2 axis of the cluster with respect to the plane of the ligand differs. In the first design strategy, the 2-fold axis of the tetrahedron is intended to lie in the same plane as that defined by the ligand (Fig. 15). Since the chelate vectors must lie within the chelate planes at each of the

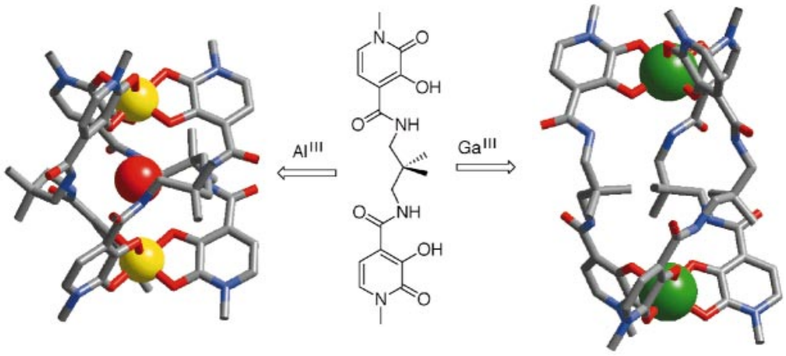

Fig. 11 Ligand H_2**13** forms both a chiral helicate (left) and an achiral mesocate (right).[77] The pictures are based on the X-ray structure coordinates. The Al_2**13**$_3$ helicate has a molecule of water in the cluster cavity similar to a previously reported iron(III) complex of a rhodotorulic acid analogue.[72]

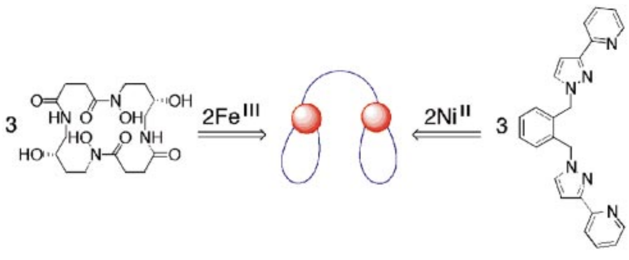

Fig. 12 The dihydroxamate siderophore alcaligin[78] (H_2**14**) and the recently reported ligand (**15**) from McCleverty and coworkers[27] form M_2L_3 clusters of the above topology with Fe(III) and Ni(II), respectively. The lines represent the ligands and the spheres represent the metal ions.

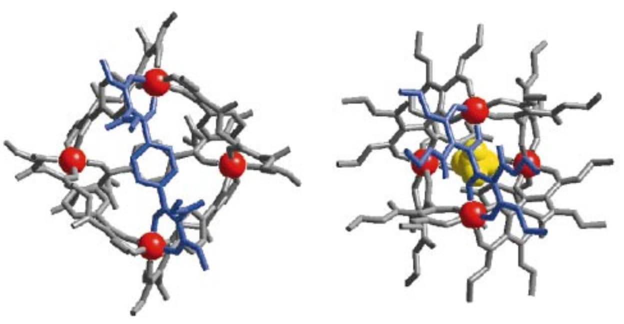

Fig. 13 As described by Saalfrank and coworkers, ligands H_2**16** (left)[79] and H_2**17** (right)[54] form M_4L_6 tetrahedral clusters with Fe(III).†† The cluster on the left has idealized S_4 symmetry, while the cluster on the right has idealized T symmetry and encapsulates a molecule of NH_4^+ (yellow).

four metal vertices, the angle between the chelate vectors within a given ligand must be 70.6°. (This angle is simply the supplementary angle to 109.4°, which is the angle between the 3-fold axes in a tetrahedron.) A 60° angle is formed for ligands H_2**18** and H_4**19** (Fig. 14); thus, the targeted structure can be achieved with only slight out of plane twisting by each of the chelating groups.

Microcrystalline precipitates of Fe_4**18**$_6$ or Ga_4**18**$_6$ were obtained from the reaction of $Fe(acac)_3$ or $Ga(acac)_3$ with H_2**18** and triethylamine in methanol.[51] Both complexes show intense peaks for the M_4L_6 molecular ions in the FAB+ mass spectrum. In addition, the crystal structure of Ga_4**18**$_6$ revealed that the tetrahedral cluster has S_4 symmetry (two Δ and two Λ metal centers) in the solid state (Fig. 16). The ligand backbone is coplanar with the S_4 axis, and there is a substantial cavity, which is partially open to the outside, in the cluster. Four crystallographically identical DMF molecules partially fill the cavity. The average carbon to carbon distance between the DMF methyl groups within the cluster cavity is 4.0 Å.

Ligand H_4**19** also appears to form a tetrahedral cluster with Ga(III) (Fig. 16).[80] The cluster $K_{12}Ga_4$**19**$_6$ precipitates from a methanol solution containing H_4**19**, $Ga(acac)_3$ and KOH after six to eight hours. The ^{1}H NMR spectrum (D_2O) of the microcrystalline product shows only one set of ligand peaks, indicating a high symmetry solution structure on the NMR timescale. In addition, preparation of the complex in the presence of excess ligand does not disrupt the formation of the desired cluster: the ^{1}H NMR spectrum of this mixture shows two sets of peaks, one for the free and one for the coordinated ligand. Unfortunately the high charge (−12) of the cluster has made obtaining X-ray quality single crystals difficult. The major ions observed in the electrospray mass spectrum (low resolution) match those expected for $[K_{14}Ga_4$**19**$_6]^{2+}$, $[K_{15}Ga_4$**19**$_6]^{3+}$ and $[K_{16}Ga_4$**19**$_6]^{4+}$.

In the second design strategy, the 2-fold axis of the tetrahedron is designed to be perpendicular to the ligand plane (Fig. 17). The ideally planar ligand should have parallel coordinate vectors that point in opposite directions. To understand this design it helps to view the tetrahedral cluster as a truncated polyhedron. If the six ligands are to act as the six 2-fold symmetric faces (shown in blue) of the polyhedron, then the angle between the chelate planes (shown in red) is no longer important. The angle between the extended 2-fold plane (blue) and the C_3 axis of the cluster is important, however, as this corresponds to the approach angle. This approach angle is 35.3° and corresponds to a perfect octahedral metal complex with a 60° twist angle. Clusters based on this design should be homochiral with idealized T symmetry (*i.e.*, all Δ or all Λ metal centers).

Ligands H_4**20**[17] and H_4**21**[81] were designed to form M_4L_6 tetrahedral clusters based on this strategy (Fig. 18). Molecular modeling[64] of the metal complexes [M = Ga(III), Fe(III)] of H_4**20** indicated that the cluster would have a substantial cavity (250–350 Å^3). Solution and solid state observations showed that one of the Et_4N^+ counterions is encapsulated within the $[M_4$**20**$_6]^{12-}$ [M = Ga(III), Fe(III)] cluster interior. The ^{1}H NMR spectrum (D_2O) of $K_5(Et_4N)_7[Ga_4$**20**$_6]$ showed two sets of Et_4N^+ resonances split in a 6:1 ratio. The larger set of Et_4N^+ peaks was shifted slightly upfield ‡‡ from free Et_4NCl (δ = 3.26, q; 1.27, t), while the smaller set was shifted *substantially* upfield, showing up at negative ppm (δ = −0.70, m; −1.59, t)! Based on literature precedent,[27,48,82–86] this extreme upfield shift was taken as an indication of the encapsulation of one Et_4N^+ cation by the tetrahedral cluster host. This assertion was further corro-

†† One of the four iron atoms in the cluster on the left is Fe(II).

‡‡ The upfield shifts of the exterior Et_4N^+ resonances are attributed to a strong π-cation interaction between the aromatic naphthalene and catechol rings of the ligands and the Et_4N^+ counterions.

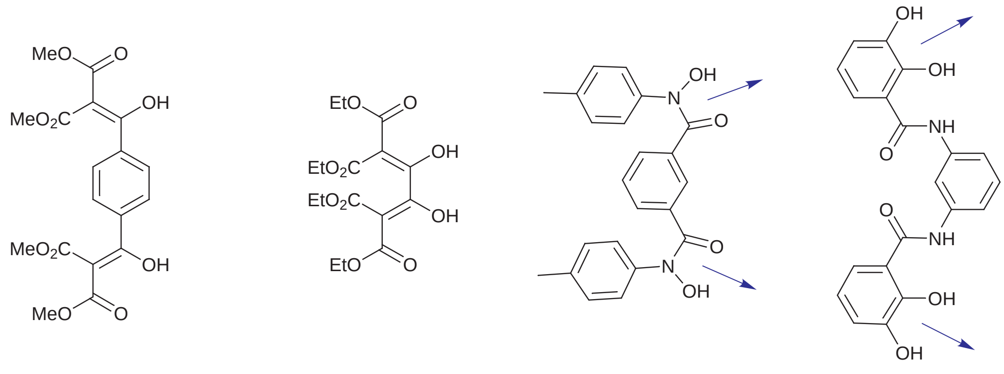

H_2**16** H_2**17** H_2**18** H_4**19**

Fig. 14 Ligands H_2**16** and H_2**17** formed M_4L_6 tetrahedral clusters as the result of fortuitous accidents. One approach to the rational design and synthesis of such clusters relies on the coordinate vectors (arrows) being 70.6° from each other. Ligands H_2**18**[51] and H_4**19**[80] form tetrahedral clusters based on this design.

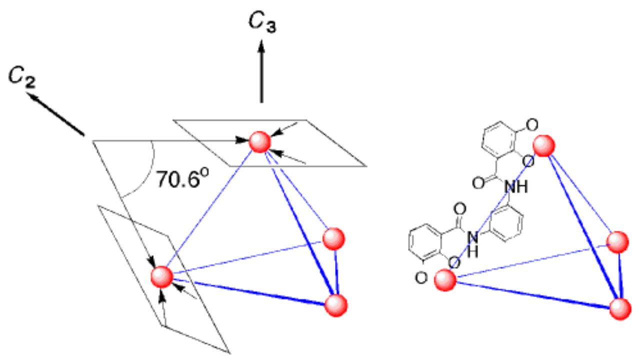

Fig. 15 One approach to the synthesis of M_4L_6 tetrahedral clusters relies on the plane of the ligand being coincident with the 2-fold axis of the tetrahedral cluster. As such, the coordinate vectors within a given ligand must be oriented 70.6° from each other.

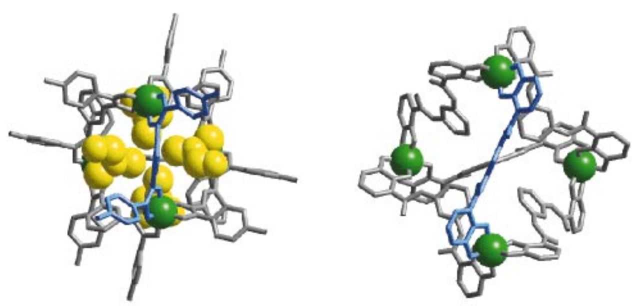

$4DMF \subset Ga_4\mathbf{18}_6$ $[Ga_4\mathbf{19}_6]^{12-}$

Fig. 16 Viewed down the crystallographic S_4 axis, the structure of $Ga_4\mathbf{18}_6$ (left) revealed four DMF solvent molecules (yellow) pointing into the cluster cavity.[51] The minimized[64,80] structure of the *T* symmetry isomer of the proposed $[Ga_4\mathbf{19}_6]^{12-}$ tetrahedron is shown (right). Notice that the highlighted ligands are nearly planar and that these planes are coincident with the 2-fold axes of the clusters.

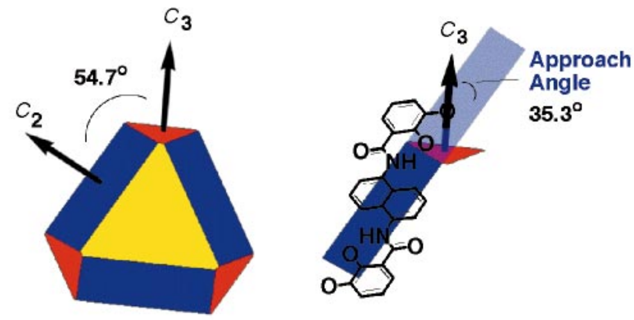

Fig. 17 One can envision an M_4L_6 cluster in which the six ligands act as the six 2-fold symmetric faces (blue) of the truncated polyhedron. This design is ideally suited for a metal center with perfect octahedral coordination (*i.e.*, approach angle = 35.3° or twist angle = 60°).

borated in the crystal structure of $K_5(Et_4N)_7[Fe_4\mathbf{20}_6]$ (Fig. 19), in which the naphthalene rings of the ligands are twisted around the arene–N bond so that they are in van der Waals contact with the encapsulated Et_4N^+. The distance between the iron atoms in the *T* symmetry cluster is 12.8 Å, bringing the cluster just into the nanometer regime.

In an attempt to make a similar cluster with a larger cavity, ligand H_4**21**, based on a 2,7-diaminoanthracene backbone, was prepared (Fig. 18). This ligand also forms an M_4L_6 tetrahedral cluster, but only in the presence of an alkylammonium guest. The ^1H NMR spectrum (D_2O) of $(Me_4N)_8[Ti_4\mathbf{21}_6]$ shows a single highly symmetric product with two Me_4N^+ resonances in a ratio of 7:1 ($\delta = 3.97$; -2.6). The presence of an extremely upfield-shifted Me_4N^+ resonance (-2.6 ppm) in a ratio of one Me_4N^+ to six ligands can be interpreted as a direct indication of the encapsulation of one Me_4N^+ by the tetrahedral cluster $[Ti_4\mathbf{21}_6]^{8-}$.[17,27,48,82–86] Again, this conclusion was corroborated in the crystal structure of $(Me_4N)_8[Ti_4\mathbf{21}_6]$ (Fig. 20); one molecule of Me_4N^+ is located in the cavity of the *T* symmetry cluster. The distance between the titanium atoms averages 16.1 Å.

However, in the absence of an alkylammonium guest molecule, H_4**21** forms an M_2L_3 triple helicate with Ti(IV) (Fig. 20).[81] Although the metal centers within a given complex have the same chirality, the overall structure is significantly distorted from idealized D_3 geometry. The local pseudo-C_3 axes at the two metal centers are not aligned, and two of the anthracene rings are oriented with their edges directed into the cluster interior, while the third anthracene ring is oriented approximately perpendicular to the plane bisecting the two former anthracene ring planes. This third ligand is substantially nonplanar. It is apparent that the greater bridge length and flexibility of the anthracene ligand allows for the formation of the M_2L_3 structure, but just barely.

Other recently reported *T* symmetry M_4L_6 tetrahedral clusters illustrate the generality of the incommensurate symmetry interaction design strategy (Figs. 18 and 19). McCleverty and coworkers[27] synthesized ligand **15**, which forms a tetrahedral cluster with Co(III). Solution and solid state evidence indicate that a molecule of BF_4^- is encapsulated in the cluster cavity. Although the ligand backbone is perpendicular to the ends of the ligand, the two chelating ends are essentially coplanar and perpendicular to the pseudo-two-fold axis of the cluster. In addition, the coordinate vectors are parallel and point in opposite directions. Another example for the utility of the design is the tetrahedral Ga(III) cluster by Stack and coworkers based on ligand H_4**22**.[37] The ligand is essentially planar and

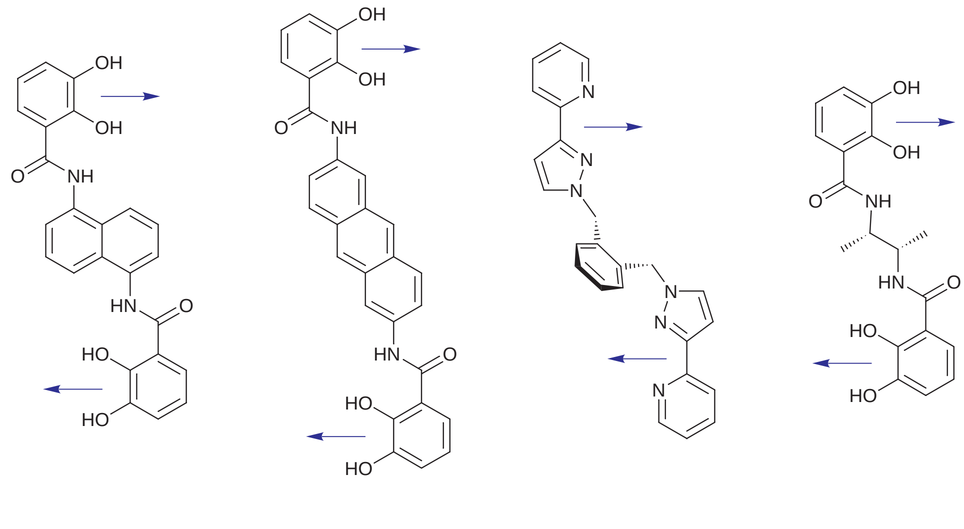

Fig. 18 Ligands H$_4$**20** and H$_4$**21** were designed to make M_4L_6 tetrahedral clusters. Based on this new design strategy, the coordinate vectors (arrows) in a ligand should be parallel and point in opposite directions. Ligands **15**[27] and H$_4$**22**[37] are recently reported examples of ligands that form tetrahedral M_4L_6 clusters and illustrate this design strategy.

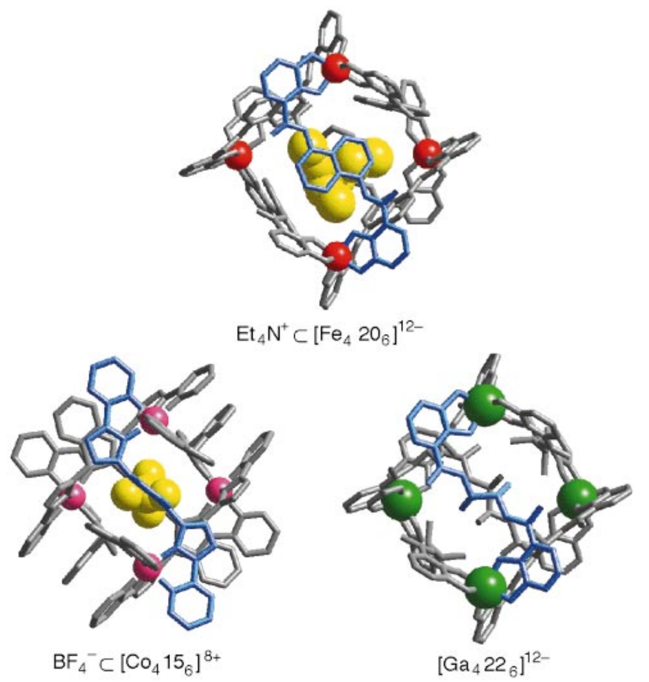

Fig. 19 H$_4$**20** forms an M_4L_6 tetrahedral cluster with Ga(III) and Fe(III). The crystal structure of the $[Fe_4\mathbf{20}_6]^{12-}$ cluster is shown at the top with the encapsulated Et_4N^+ shown in yellow. Ligands **15** and H$_4$**22** also form M_4L_6 tetrahedral clusters with Co(II) and Ga(III), respectively. The crystal structures of $BF_4^- \subset [Co_4\mathbf{15}_6]^{8+}$ (bottom left)[27] and $[Ga_4\mathbf{22}_6]^{12-}$ (bottom right)[37] are shown. Note the similarity of the conformation of the highlighted ligand in each structure: the ligands are nearly planar, and the coordinate vectors are parallel and point in opposite directions.

perpendicular to the pseudo-two-fold axis of the *T* symmetry cluster. Again, the parallel coordinate vectors point in opposite directions.

M_4L_4 Complexes

An approach to the synthesis of M_4L_4 tetrahedral clusters has also been developed. In an M_4L_4 tetrahedral cluster the metal ions occupy the four vertices and the ligands occupy each of the four faces of the tetrahedron (Fig. 21). This implies that both the ligand and the metal ion must have 3-fold symmetry. As in the previously described M_2L_3 helicates and M_4L_6 tetrahedra, three bidentate ligands coordinating a pseudo-octahedral metal ion can generate a 3-fold axis at the metal. Rather than using a C_2-symmetric ligand, a C_3-symmetric ligand can be utilized. This ligand must be rigid, however, so that no two chelating moieties on the ligand can coordinate a single metal ion. Ligand H$_6$**23** satisfies this requirement (Fig. 21).[18]

If the ligand is ideally planar, as in the case of H$_6$**23**, then the approach angle for this type of cluster is 19.4° (Fig. 22). This ideal angle is less than four degrees from the approach angle of 23° (corresponding twist angle = 40°) observed for tris-(catecholate) complexes of Ti(IV), Ga(III) and Fe(III);[56,61,87] therefore, this design seems optimized for metal ions with significant distortions toward trigonal prismatic geometry.

Ligand H$_6$**23** reacted with Al(III), Fe(III) and Ga(III) under basic conditions to give precipitates whose ^{1}H NMR and mass spectra indicated the expected M_4L_4 species.[80] The high charge (12−) of these clusters precluded the isolation of X-ray quality single crystals, however, because of the large number of countercations to be ordered in a crystalline lattice. The use of higher oxidation state metal ions [*e.g.*, Ti(IV) and Sn(IV)], despite reducing the lability of the metal–ligand system, would lower the overall charge of the cluster to 8−, thus reducing the number of countercations. With this in mind, the Ti(IV) and Sn(IV) complexes of H$_6$**23** were prepared, and X-ray quality crystals were obtained of the $(Et_3NH)_8[Ti_4\mathbf{23}_4]$ complex (Fig. 22).[18] The cluster is a racemic mixture of homochiral tetrahedra (either all Δ or all Λ configuration within a given cluster). There is no evidence that the small cavity of the tetrahedron contains a guest, as observed in the previously described M_4L_6 clusters.

The manganese(II) cluster reported by McCleverty and coworkers using ligand **24** further illustrates that a 3-fold symmetric tris(bidentate) ligand can be used to synthesize homochiral M_4L_4 tetrahedral clusters by self-assembly (Fig. 23).

Two metal clusters

We have recently demonstrated the rational design of a $M_2M'_3L_6$ mixed-metal cluster in which, rather than using a symmetric *ligand* to generate a symmetry element, two *different metals* generate the two incommensurate symmetry elements (Fig. 24).[89] In principle, the ligand H$_2$**25** forms part of an asymmetric unit of the cluster and must have two different incommensurate symmetry interaction sites. As described earlier, a chiral triple helicate has idealized D_3 symmetry, while

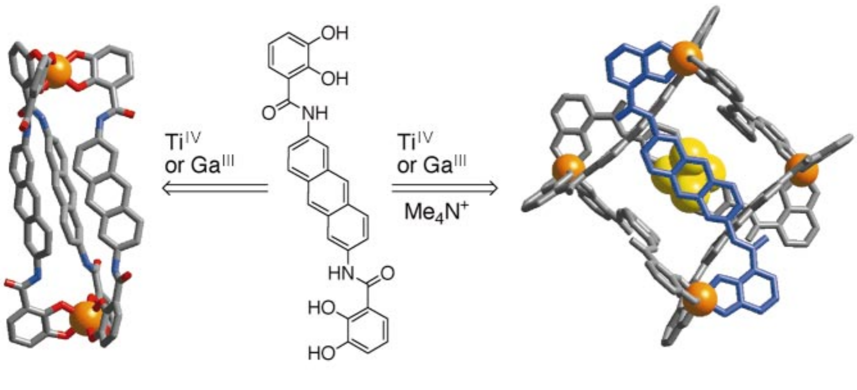

$[Ti_2\mathbf{21}_3]^{4-}$ $H_4\mathbf{21}$ $Me_4N^+ \subset [Ti_4\mathbf{21}_6]^{8-}$

Fig. 20 Ligand $H_4\mathbf{21}$ forms an M_2L_3 helicate in the absence of a Me_4N^+ guest, but an M_4L_6 tetrahedron in the presence of Me_4N^+. The crystal structures of $[Ti_2\mathbf{21}_3]^{4-}$ (left) and $Me_4N^+ \subset [Ti_4\mathbf{21}_6]^{8-}$ (right) are shown.[81]

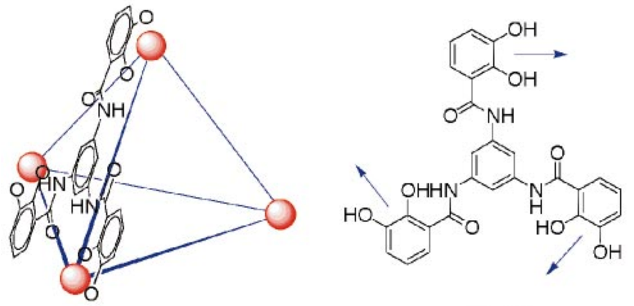

$H_6\mathbf{23}$

Fig. 21 An M_4L_4 tetrahedral cluster with the metals on the vertices and ligands on the faces of the tetrahedron can be synthesized using ligand $H_6\mathbf{23}$.

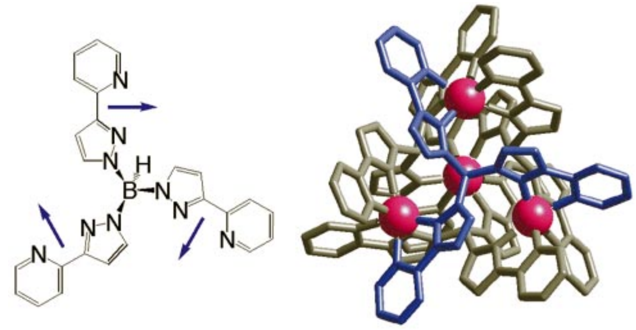

24 $[Mn_4\mathbf{24}_4]^{4+}$

Fig. 23 McCleverty and coworkers reported the M_4L_4 tetrahedron $[Mn_4\mathbf{24}_4]^{4+}$. The manganese atoms are ferromagnetically coupled.[88]

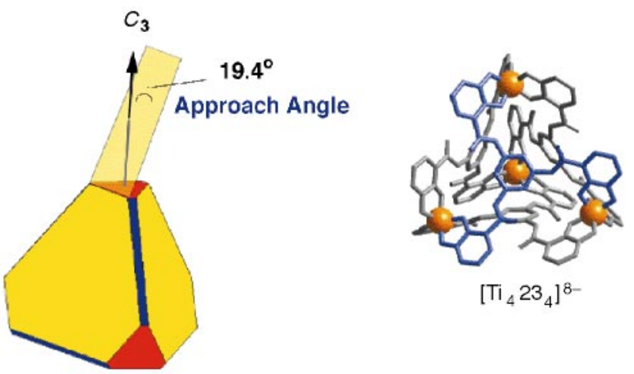

Fig. 22 If the ligand is ideally planar, as in the case of $H_6\mathbf{23}$, then the angle that the 3-fold face (yellow) of the tetrahedron makes with the C_3 axis is 19.4° and corresponds to the approach angle. The crystal structure of $[Ti_4\mathbf{23}_4]^{8-}$ is shown (right).[18]

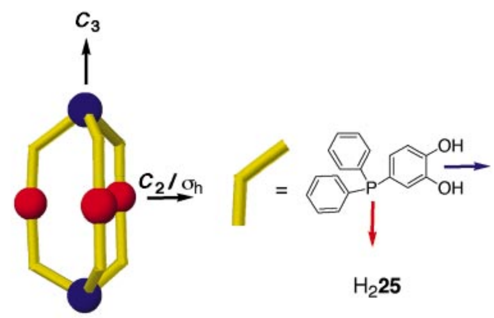

Fig. 24 A cluster with D_3 (or C_{3h}) symmetry can be designed using an asymmetric ligand $H_2\mathbf{25}$.[89] Interaction of the catechol moiety with an octahedral metal ion (blue spheres) can generate the necessary C_3 axis, while interaction of the phosphine moiety with a square planar metal ion (red spheres) can generate the C_2 axis (or mirror plane). Simultaneous satisfaction of these two symmetry requirements can lead to a cluster with D_3 (or C_{3h}) symmetry.

an achiral triple mesocate has C_{3h} symmetry. Therefore, to synthesize a mixed-metal helicate (or mesocate) of stoichiometry $M_2M'_3L_6$, one must consider a three-fold interaction site and an orthogonal two-fold (mirror plane) interaction site (Fig. 24).

As already illustrated, catechol ligands are relatively hard donors and generate a C_3 axis when forming a tris-chelate with hard, trivalent or tetravalent metals [*e.g.*, Al(III), Ga(III), Fe(III), Sn(IV), Ti(IV)].[56,59,61,90,91] Phosphine ligands, on the other hand, are soft donors and can generate a two fold axis or mirror plane when coordinated to a square planar metal [*e.g.*, Pd(II) or Pt(II)] in a *trans* fashion.[92,93] A ligand containing both these functionalities arranged in the proper geometry can assemble a $M_2M'_3L_6$ cluster, because it is the smallest discrete species that would simultaneously fulfill the two orthogonal symmetry requirements.

The crystal structure of $Cs_4[Ti_2\mathbf{25}_6(PdBr_2)_3]$ shows that the complex has C_{3h} symmetry (Fig. 25); the cluster is a mesocate with one of the titanium atoms having Δ- and the other having Λ-configuration. Significantly, three of the Cs^+ counterions are located in clefts of the cluster (Fig. 25). Each is coordinated by four of the catecholate oxygens and two molecules of THF. The clefts of the cluster are so deep that the coordinating THF molecules can also be described as being buried. The palladium-coordinated bromine atoms are not in van der Waals contact with the caesium atoms, but they do shield the caesium atoms from other solvent molecules, helping to explain the low coordination number (6) of the Cs^+ cations.

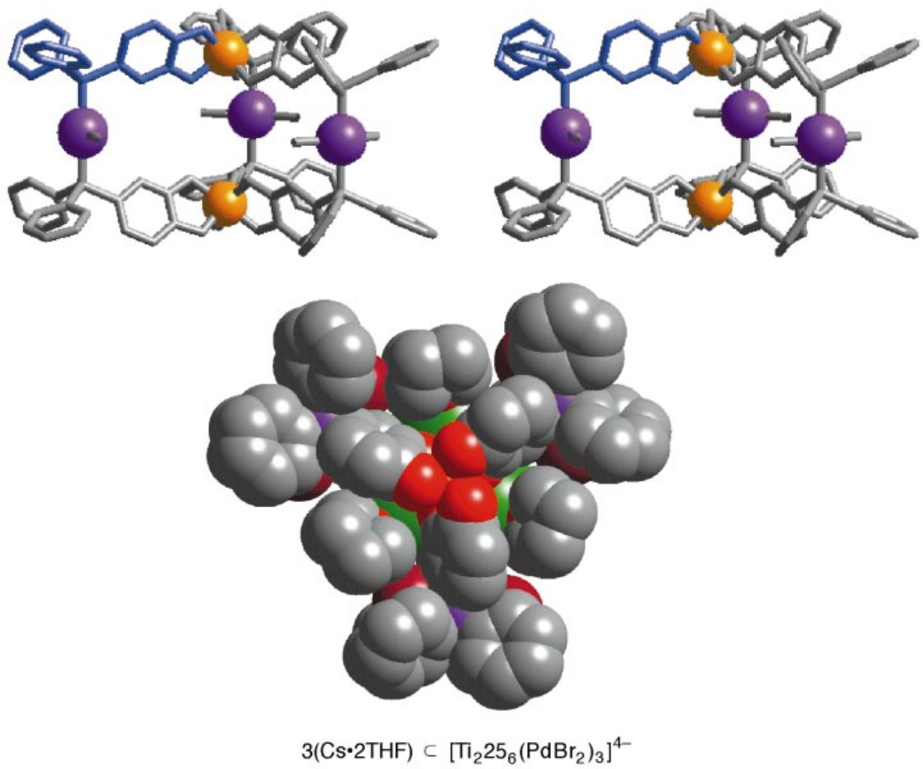

Fig. 25 In the stereoview (top) of $[Ti_2\mathbf{25}_6(PdBr_2)_3]^{4-}$ the Pd atoms are colored purple and the titanium atoms are colored orange. Viewed down the crystallographic 3-fold axis, this space filling model shows the buried caesium cations (green) and their coordinated THF molecules. The hydrogen atoms are omitted for clarity.[89]

$m(M_xL_y)$ *versus* $n(M_xL_y)$ clusters

Especially with high symmetry structures, it is imperative to have molecular weight data if structure assignment is to be certain, as there are several examples of ligands that make clusters of both $m(M_xL_y)$ and $n(M_xL_y)$ stoichiometries. McCleverty and coworkers reported that ligand **15** makes an M_4L_6 tetrahedron with Co(II) but an M_2L_3 alcaligin-type cluster with Ni(II) (Figs. 12, 18 and 19).[27] We have reported that ligand H$_4$**21** makes an M_4L_6 tetrahedron in the presence of an alkylammonium guest but an M_2L_3 triple helicate in the absence of guest (Fig. 20).[81] Lehn and coworkers have reported both penta- and hexanuclear circular helicates of Fe(II) using ligand **26**; in the absence of a Cl^- guest the hexanuclear circular helicate forms, while in the presence of Cl^- the pentanuclear helicate forms (Fig. 26).[42] It has been similarly suggested that molecular "squares" (**27**) are in equilibrium in solution with molecular "triangles" (**28**) as shown in Fig. 27.[31,94] In each of the above examples, the metal–ligand ratio is the same between the two structures, and therefore spectroscopic evidence or analytical data is of limited value. Only high resolution mass spectrometry or X-ray diffraction data could distinguish between an $m(M_xL_y)$ or an $n(M_xL_y)$ structure.

Recently Stang and coworkers reported the synthesis of a nanoscale molecular hexagon (**29**, Fig. 27).[39] Characterization of this compound included spectral and analytical results, but did not include mass spectrometry or crystallographic data. The formulation of the complex as a hexagon was based on the use of a linker with a 120° bond angle. The discrepancy between the 120° angle needed for a hexagon and the 108° angle needed for an analogous pentagon, for example, is easily accounted for when one considers the size of the molecule. One edge of either of these macrocycles is over 23 Å. This includes seven angles that, when compared to analogous angles taken from the Cambridge Structural Database,[95] would be expected to deviate from the ideal by two to three degrees each. This is more than enough to make up for the necessary 12° per edge. Even the previously reported "molecular square", based on 90° angles, has corner angles around square planar platinum of 83°.[96] Independent molecular modeling[64] of both the hexagon (**29**)

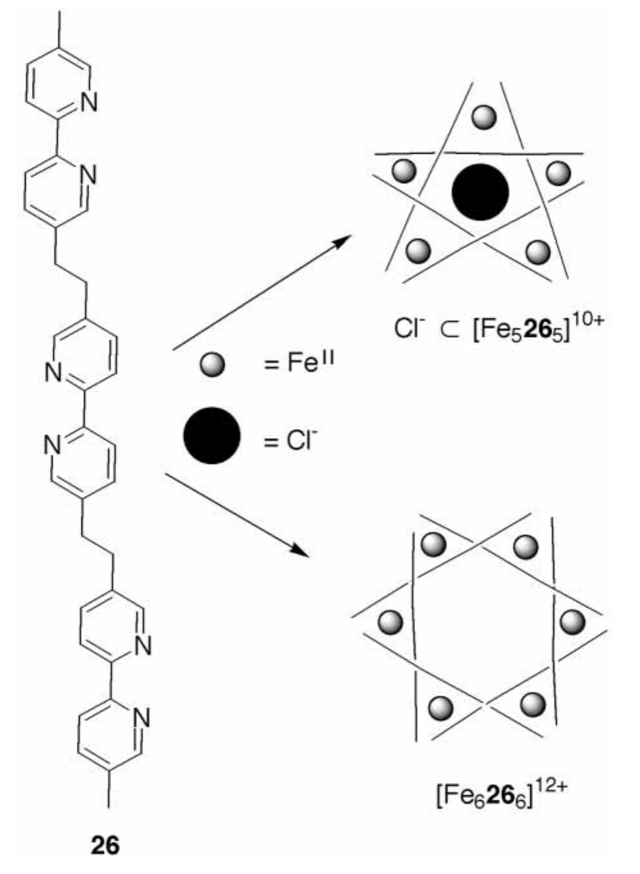

Fig. 26 Lehn and coworkers reported that the hexadentate bipyridine ligand **26** shown above makes a pentanuclear $[Fe_5\mathbf{26}_5]^{10+}$ circular helicate with Fe(II) in the presence of the guest Cl^-, but a hexanuclear $[Fe_6\mathbf{26}_6]^{12+}$ circular helicate in the absence of Cl^-.[42]

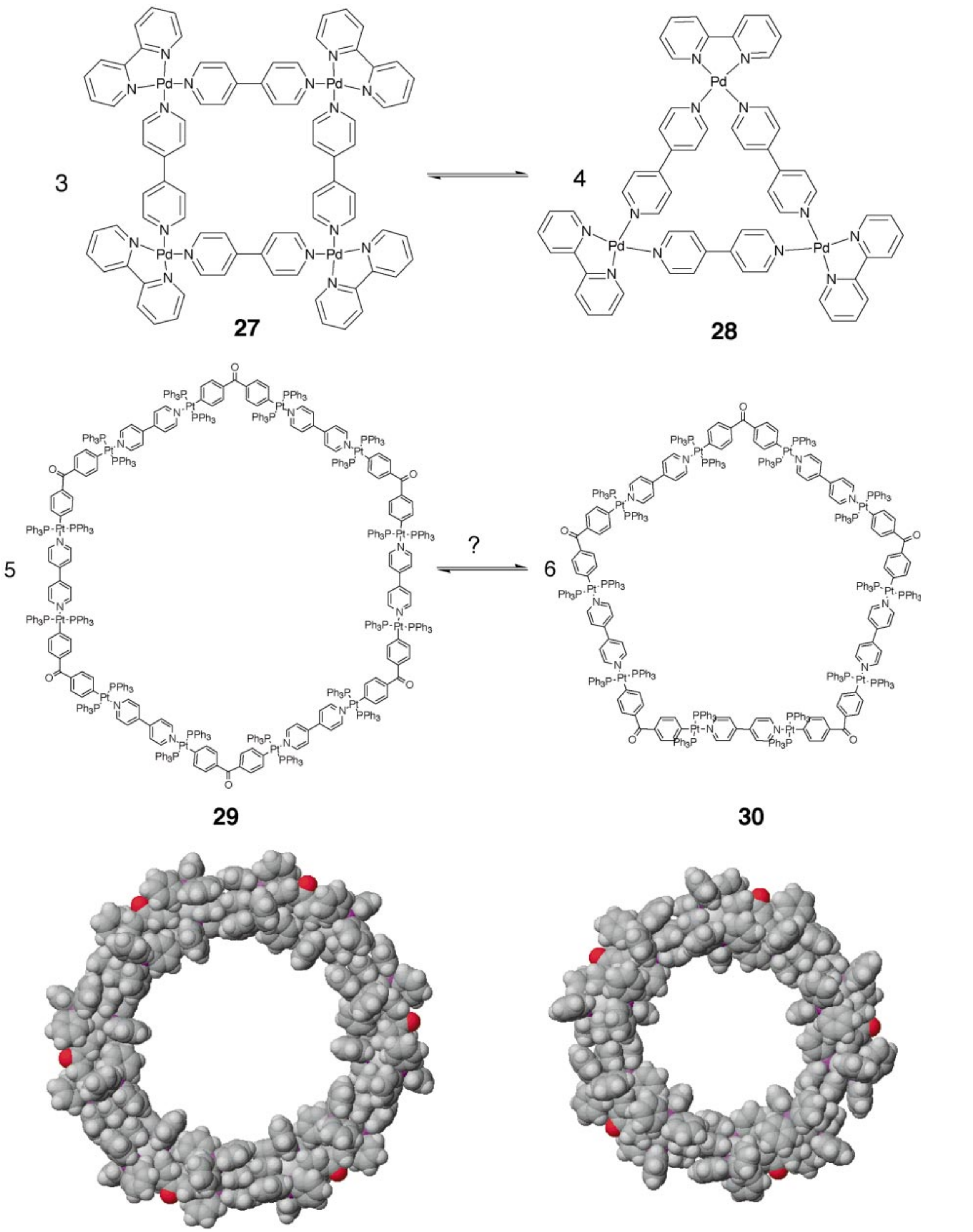

Fig. 27 Fujita and coworkers have presented evidence that suggests the molecular "square" (**27**) and "triangle" (**28**) shown above are in equilibrium in solution.[94] Stang and coworkers have suggested that the molecular "hexagon" (**29**) exclusively forms from the ligand and metal components based on the use of a linker with a 120° angle.[39] Independent molecular modeling[64] of both the proposed hexagon and an analogous pentagon reveal no obvious steric interactions that would cause the hexagon to be favored over the pentagon.

and the pentagon (**30**) revealed no obvious steric interactions or strain around the metal centers in either proposed structure (Fig. 27). While NMR data can point to the existence of a symmetric structure, and both NMR and elemental analysis can determine metal–ligand or ligand–ligand′ ratios, only mass spectrometry or crystallographic data can give the full formula and structure.

Dynamics of supramolecular clusters

The geometric requirements for synthesizing clusters of various stoichiometries and symmetries are beginning to be understood. It is less clear, however, how these clusters assemble in solution from the ligand and metal components, and once assembled, how the clusters function. For example, how is

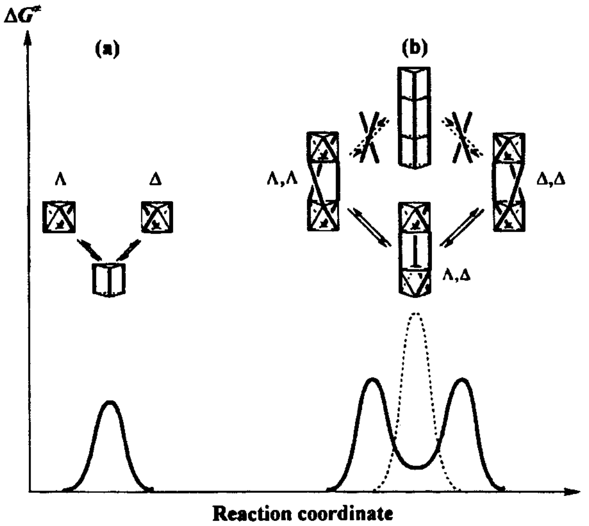

Fig. 28 Potential energy diagrams and stereochemical courses for intramolecular inversion of (a) the mononuclear complex and (b) the Λ,Λ-$[Ga_2\mathbf{8}_3]^{6-}$ and Δ,Δ-$[Ga_2\mathbf{8}_3]^{6-}$ dinuclear complexes involving the heterochiral Λ,Δ-$[Ga_2\mathbf{8}_3]^{6-}$ as an intermediate (solid lines). Inversion with a hypothetical, concerted twisting of both metal centers is indicated by a dashed line.

geometric information transmitted between the multiple coordination sites of a given ligand? Is there coupling of the isomerization of chiral metal centers and, if so, what is the magnitude of this coupling as transmitted through the rigid ligand? For clusters that recognize and encapsulate guest molecules, what are the factors controlling the recognition process and how do guests enter and exit the cluster cavity?

M_2L_3 Triple helicate stereo-isomerism dynamics

When using rigid ligands to synthesize triple helicates, the chirality of the first metal center should induce the same chirality at the second metal center, so that only ΔΔ- and ΛΛ-configured complexes are present. The magnitude of the mechanical coupling between the two metal centers and the mechanism of the inversion reaction have been investigated using the dinuclear Ga(III) complexes of ligands $H_4\mathbf{8}$–$H_4\mathbf{10}$ and similar mononuclear Ga(III) complexes based on simple bidentate catecholamide ligands.[65,66,97] The methyl groups on the isopropyl substituents of $H_4\mathbf{8}$ are magnetically equivalent in the free ligand, but become magnetically inequivalent around the chiral metal center.

The activation parameters for this process were derived from an Eyring plot of the first-order rate constants calculated by line shape analysis. Consistent with an intramolecular mechanism, these parameters are not solvent dependent. The free energy inversion barrier ($\Delta\Delta \longleftrightarrow \Lambda\Lambda$) for $K_6[Ga_2\mathbf{8}_3]$ in DMSO-d_6 (79.8 kJ mol^{-1}) or D_2O solutions (78.7 kJ mol^{-1}, pD = 12.1) is only 1.2 times higher compared to the corresponding mononuclear complex. Two limiting cases for coupling of the two metal centers and their chirality can be considered: for weak coupling the barrier should remain essentially unchanged. However, for very strong coupling the two centers must move through the trigonal-prismatic transition state simultaneously (Fig. 28), and consequently the activation barrier would be expected to be effectively twice the barrier for inversion of the mononuclear complex. The kinetic data show weak coupling of both metal centers that is about 22.6 kJ mol^{-1}. Thus, it is concluded that inversion of the Λ,Λ- and Δ,Δ-$[Ga_2\mathbf{8}_3]^{6-}$ helicates involves the heterochiral Λ,Δ-$[Ga_2\mathbf{8}_3]^{6-}$ anion as an intermediate, which is produced by a single twist event along the reaction pathway.

At lower pD a second mechanism becomes dominant in D_2O. In contrast to the mononuclear complex, the dinuclear $K_6[Ga_2\mathbf{8}_3]$ helicate shows a second order proton dependence below pD = 7. This constitutes a remarkable confirmation of the mechanism outlined in Fig. 28: inversion of one center, which occurs rapidly because of the single protonation, does not change the overall chirality owing to the higher energy of the heterochiral intermediate and its consequent short lifetime. Only when the second metal center is also protonated can the overall inversion of the helicate occur. In the absence of mechanical coupling of the metal centers only a single proton dependence would be expected because the heterochiral intermediate would have the same energy as the homochiral anions and, consequently, a long lifetime.

rac-(ΔΔ/ΛΛ)-M_2L_3 Helicate to ΛΔ-M_2L_3 mesocate interconversion dynamics

As noted earlier, in the solid state $H_2\mathbf{13}$ forms a helicate with Al(III) but a mesocate with Ga(III) (Fig. 11).[77] The methyl substituents in the $H_2\mathbf{13}$ backbone serve as markers for following the solution structure of the metal complexes by ^1H NMR; in the helicate these two methyl groups are equivalent, while in the mesocate the methyl groups are diastereotopic. As expected for the mesocate, the ^1H NMR spectrum of $Ga_2\mathbf{13}_3$ in DMSO-d_6 shows two singlets for the methyl groups in the ligand spacer; however, the presence of an additional singlet indicates that the helicate form of this complex is also present in solution. Variable temperature ^1H NMR experiments reveal that these two structures are in thermodynamic equilibrium, with the helicate being preferred at high temperatures. Additional investigations revealed that the spontaneous *meso*-to-helix conversion is an entropy-driven process, which must be a consequence of different numbers of solvent molecules associated with the two forms of the complex.[77] While $Al_2\mathbf{13}_3$ also displays dynamic behavior, it is considerably slower than the corresponding Ga(III) complex. It has been previously shown that inversion of Ga(III) helicates is fast on the NMR time scale and proceeds through an intramolecular Bailar twist.[65,66,97] Inversion of configuration in mononuclear Al(III) and Ga(III) complexes proceeds through the same mechanism,[98,99] and the isomerization or exchange rates for Ga(III)-trischelates are consistently faster than for Al(III)-trischelates.[100]

Stereoisomerism in M_4L_6 tetrahedral clusters

As described, the M_4L_6 tetrahedral cluster based on ligand $H_2\mathbf{18}$ crystallizes as the S_4 isomer (ΔΔΛΛ chiralities at the four metal vertices).[51] Low temperature ^1H NMR experiments reveal, however, that $Ga_4\mathbf{18}_6$ is a mixture of T (ΔΔΔΔ/ΛΛΛΛ), C_3 (ΔΛΛΛ/ΛΔΔΔ) and S_4 (ΔΔΛΛ) isomers in solution ($CDCl_3$).[20] With decreasing temperature the broad resonance of one of the ligand protons, which is pointing into the cavity, splits into five distinct peaks, representing the three isomers.

The integration of the peaks at 220 K yields a ratio of C_3:S_4:T isomers of 58:38:4. If the distribution between the isomers were purely statistical, one would expect the ratio of C_3:S_4:T isomers to be 50:37.5:12.5. Although the isomers are not present in an exact statistical distribution, the distribution shows that the stabilities of the three isomers are very similar, and, therefore, the mechanical coupling between the metal centers is negligible.

Ligand exchange in hydroxamate iron(III) complexes has been previously studied,[58] but isomerization of a simple tris-hydroxamate iron(III) or gallium(III) complex is certainly too fast to follow by NMR. The slower rate of interconversion detected here can be attributed to the geometric properties of the ligand and the cluster. In order for a metal center to change its chirality it is necessary to pass through a trigonal prismatic transition state. Since four coordination centers are tethered in the tetrahedron, the Bailar twist is the only mechanically possible rearrangement. To do this, the ligands in contact with the active metal *must* pass through a conformation in which the

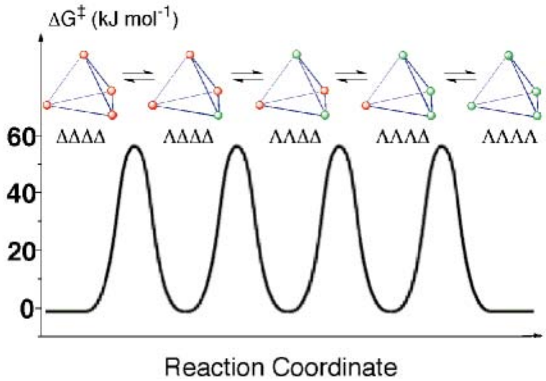

Fig. 29 Potential energy diagram and stereochemical courses for intramolecular inversion of the T symmetry (ΛΛΛΛ/ΔΔΔΔ), C_3 symmetry (ΛΛΛΔ/ΔΛΛΛ) and S_4 symmetry (ΛΛΔΔ) isomers of Ga_4**18**$_6$.

ligand's two coordinate vectors can not coexist in the chelate planes of each metal center. In effect, because the ligand maintains an angle of only 60° in its planar form it forces a very distorted trigonal prismatic intermediate.

The stereochemical courses and potential energy diagram for the isomerization of ΔΔΔΔ to ΛΛΛΛ cluster are drawn in Fig. 29. In order to isomerize from ΔΔΔΔ to ΛΛΛΛ, the cluster has to go through all intermediate stereoisomers. Since both NMR observations and MM2 calculations suggest that all these isomers are very close in energy, they are drawn here at the same energy level. The potential energy diagram can be then simplified if we assume that isomerization of ΔΔΛΛ to ΔΔΔΛ will have the same energy barrier as its isomerization to ΔΛΛΛ, since both processes require inversion of configuration at only one metal center. The inversion from ΔΔΔΛ to ΔΔΔΔ must have the same energy barrier as inversion of ΔΛΛΛ to ΛΛΛΛ, since these are mirror image processes. Coalescence of the ^{1}H NMR resonances is observed at 300 K, corresponding to an activation barrier of 58 kJ mol^{-1}.

Self-recognition in M_2L_3 triple helicates

A different issue of designed order was addressed in a family of helicate complexes of varying, but fixed, metal–metal distance. It was intended that the information stored in rigid bis(catecholamide) ligands (H_4**4**–H_4**6**, Fig. 7) be used to overcome the intrinsic disorder of mixtures to produce a highly ordered system of complexes in solution. These ligands are unique in that, because of the rigidity and varying distances between the catecholamide functionalities, it is geometrically impossible to form a mixed ligand $(M_2L_2L'_1)^{6-}$ complex. There are few synthetic examples of self-recognition, despite nature's ability to perform this feat in many ways. Lehn and coworkers have demonstrated the self-recognition of double stranded copper(I) helicates that differ in the number (2–5) of metal coordination sites.[101] More recently Stack and coworkers have shown that racemic mixtures of chiral ligands stereoselectively form complexes in which all ligands are of the same chirality.[37,102]

When mixtures of any two or all three of the ligands shown in Fig. 7 are equilibrated at room temperature with $Ga(acac)_3$ in basic methanol, both ^{1}H NMR spectroscopy and electrospray mass spectrometry indicate that only the individual complexes form (Fig. 30). Remarkably, no oligomeric or mixed-ligand species are observed in solution.

Selective encapsulation of alkylammonium guests by a tetrahedral cluster host

The tetrahedral cluster $[Ga_4$**20**$_6]^{12-}$ shows remarkable discrimination between alkylammonium guests.[17] There are orders of magnitude differences between the association equilibrium

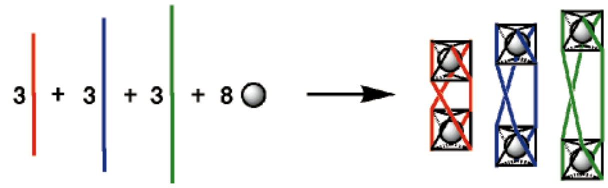

Fig. 30 Schematic representation of self-recognition in gallium(III) triple helicates. The different sized rods represent the different length ligands. Spheres represent the gallium ions.

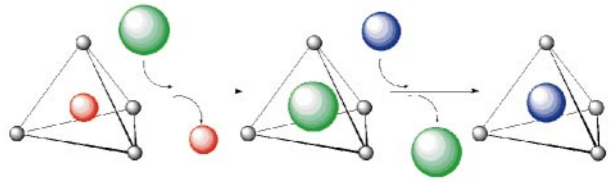

Fig. 31 Schematic representation of stepwise guest exchange from the cavity of the tetrahedral cluster $[Ga_4$**20**$_6]^{12-}$. The red spheres represent Me_4N^+, the green spheres Pr_4N^+ and the blue spheres Et_4N^+.

constants, K_{eq}, for Me_4N^+, Et_4N^+ and Pr_4N^+, and these differences allow for the quantitative step-wise exchange of one guest for another (Fig. 31). If Pr_4N^+ is added to a solution of $K_6(Me_4N)_6[Ga_4$**20**$_6]$, the Pr_4N^+ quickly (<1 min) and quantitatively is incorporated into the cluster cavity, displacing Me_4N^+. In turn, if Et_4N^+ is added to this same solution, the Et_4N^+ displaces the Pr_4N^+ rapidly (<1 min) and quantitatively! In the presence of either Me_4N^+, Et_4N^+ or Pr_4N^+, the tetrahedral cluster selectively encapsulates Et_4N^+. No mixtures are observed by ^{1}H NMR.

The thermodynamic parameters for the inclusion reaction in water have been determined by measuring the temperature dependence of the association equilibrium constants (K_{eq}).[82] Since the exchange between free and encapsulated guests is slow on the NMR time scale, their relative concentrations can be determined by integration of the corresponding ^{1}H NMR resonances. In the absence of any other guests the cavity of the $[Ga_4$**20**$_6]^{12-}$ host will most likely be filled with solvent molecules. Both ^{39}K NMR spectroscopy and the lack of a K^+ concentration dependence on the equilibrium values suggest that the K^+ cations are located outside the cavity and do not interact with the interior of the cluster.

The van't Hoff plots for the encapsulation of $Me_2Pr_2N^+$, Pr_4N^+ and *N*,*N*,*N′*,*N′*-tetramethyl-1,3-propanediammonium by the host $[Ga_4$**20**$_6]^{12-}$ anion show that encapsulation of the cationic guests into this dodecaanion is an *endothermic* process. The enthalpies and entropies are both positive; the encapsulation is an entropy-driven process.

Encapsulation of a cation by a dodecaanion is endothermic due to the very large, and dominant, solvation enthalpies of the ions (Fig. 32). The free energy of hydration is predicted by the Born equation to be $-162\, z^2 r^{-1}$ kcal mol^{-1}, where z are units of charge and r the diameter of the ion in Å.[103] The corresponding entropy of hydration is $-2.8\, z^2 r^{-1}$ kcal mol^{-1} at 298 K, predicting a ΔH of hydration of $-165\, z^2 r^{-1}$ at 298 K. Because ΔH of hydration is z^2 dependent, solvation of the -12 anion is the largest term. This and the cation solvation override the enthalpy gained on partial charge neutralization. This model also makes a clear prediction that higher charge cations will not be encapsulated and that highly solvated, singly charged cations (*i.e.*, K^+) should be poor guests. These predictions are confirmed by the observed behavior.

The major entropy terms in the host–guest complexation reaction are all positive. A large entropy gain upon host–guest complexation is predicted based both on desolvation of the ions and release of encapsulated water by the host (Fig. 33). This model is consistent with other examples of ion pairing or com-

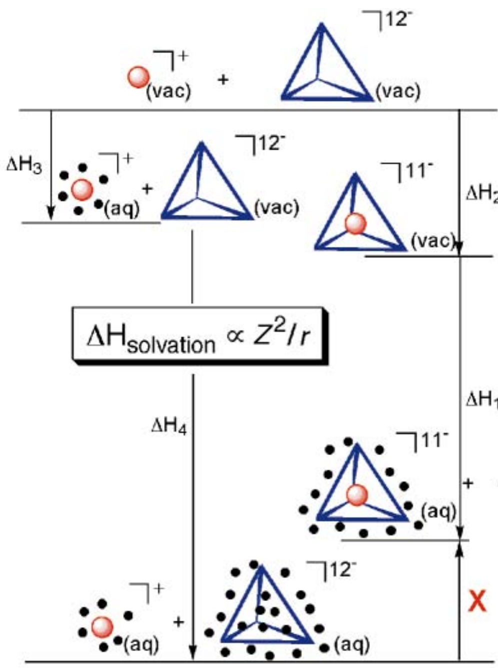

Fig. 32 Born–Haber cycle for guest encapsulation by $[Ga_4\mathbf{20}_6]^{12-}$. Solvation of the negative twelve anion is the largest enthalpy term (ΔH_4) because of the z^2 dependence of solvation enthalpy. The enthalpy of the encapsulation event in aqueous solution (denoted by a red X) was determined experimentally.

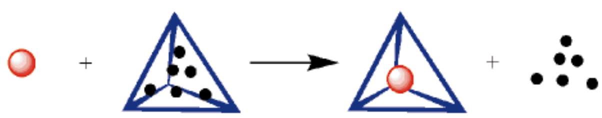

Fig. 33 Upon encapsulation of the guest, the "frozen" solvent molecules in the cluster cavity are released, resulting in a favorable entropy gain.

plexation of metallic ions with anionic ligands, which are also entropically driven processes.[104]

We have further investigated the role of solvent by measuring the thermodynamic parameters of the encapsulation of alkylammonium cations by the tetrahedral cluster $[Ga_4\mathbf{20}_6]^{12-}$ in various solvents.[105] The ΔG values for the encapsulation event show excellent correlation with several empirical scales that describe the polarity of the solvent, suggesting that the selectivity and extent of inclusion depends on the solvation of the dodecaanionic host and the cationic guest.

Guest-induced M_2L_3 helicate to M_4L_6 tetrahedron conversion

We have shown that two different clusters,[81] a triple helicate and a tetrahedron, can be prepared using identical ligand ($H_4\mathbf{21}$) and metal components (Fig. 20).[27,37,42,43,106–109] Simply the addition of an appropriate guest is enough to shift the equilibrium from the entropically preferred helicate to the tetrahedron. Since the only difference in the two systems described above is the presence or absence of Me_4N^+, it should be possible to transform a triple helicate into a tetrahedral cluster simply upon addition of Me_4N^+. In order to test this hypothesis, the Ga(III) analogues were prepared because of the greater lability of Ga(III) compared to Ti(IV). The addition of 20 equivalents of Me_4NCl to a $K_6[Ga_2\mathbf{21}_3]$ solution in D_2O revealed that this was indeed possible. Complete transformation of the helicate into the tetrahedral cluster was observed *via* ^{1}H NMR spectroscopy over the course of 5 days (pD 6.5, T 40 °C). Similar studies of this transformation at higher pD values (pD 7.5) and lower temperatures (room temperature) showed lower conversion rates due to the slower kinetics of metal–ligand rearrangement under these conditions.

Summary

In this review we have illustrated the utility and generality of an approach to the *designed* synthesis of supramolecular clusters based on metal–ligand interactions. An analysis of the high symmetry seen in the natural protein clusters (*e.g.*, ferritin and viral protein coats) is based on the incommensurate symmetry numbers of the interaction sites and the fixed relative angles between these symmetry axes. The use of this model in the successful design of several metal–ligand clusters is illustrated. Rigid ligand geometries, while chosen to accommodate the targeted cluster geometry, preclude the formation of alternative structures. This process is greatly facilitated by molecular modeling in the early stages of design.

Triple helicates of M_2L_3 stoichiometry are based on bis(bidentate) ligands with C_2 symmetry interacting with "octahedral" metal centers that generate C_3 axes when coordinated by three bidentate chelators. When the angle between the C_3 and C_2 axes is rigidly fixed at 90° by the use of a rigid linker between the two coordinating ends of the ligand, a chiral triple helicate is the most likely structure. When less rigid linkers are used, achiral mesocates and even alcaligin-type topologies are increasingly possible.

Tetrahedral clusters of M_4L_6 stoichiometry are similarly based on bis(bidentate) C_2-symmetric ligands and "octahedral" metal centers. In contrast to the M_2L_3 helicates, when the angle between the C_3 and C_2 axes is rigidly fixed at 57.4°, a tetrahedral cluster results. Two strategies for achieving this geometry and the resulting M_4L_6 tetrahedral clusters are presented. Alternatively, M_4L_4 tetrahedra can be synthesized by imposing C_3 symmetry on the ligand, which is designed to span the face of the tetrahedron and bridge three metal vertices. In addition to illustrating these design approaches towards tetrahedral structures *prospectively* in the synthesis of numerous clusters, we have also shown *retrospectively* that several clusters reported by others conform to the geometric parameters called for by our model.

The initial investigation of the dynamic behavior of these synthetic supramolecular clusters has begun. We are beginning to understand the mechanical coupling (or lack thereof) between chiral metal centers in M_2L_3 and M_4L_6 clusters, the kinetics and host-guest chemistry of multi-metal complexes, the self-recognition properties in pre-designed rigid systems and the dramatic role that guest molecules can play in the formation of clusters of $n(M_xL_y)$ (n = 1, 2, 3, . . .) stoichiometries.

The host–guest chemistry of these clusters offers the first promise of achieving synthetically what nature accomplishes in the supramolecular clusters of ferritin and viral protein coats. In both cases the natural clusters protect valuable guest molecules by providing a nanometer scale environment that is significantly different from the surrounding solution. We have described the first indication that we can significantly alter the properties of the guest molecules in the host clusters we have prepared. The further development of the reaction chemistry of the encapsulated guests is an exciting prospect.

Acknowledgements

This research is supported by the National Science Foundation through Grant No. CHE-9709621 and exchange grants from NATO (SRG 951516) and NSF (INT-9603212). We thank Darren W. Johnson for his help with manuscript preparation.

References

1 J.-M. Lehn, *Supramolecular Chemistry: Concepts and Perspectives*, VCH, Weinheim, 1995.
2 P. M. Harrison and P. Arosio, *Biochim. Biophys. Acta*, 1996, **1275**, 161.
3 P. M. Proulxcurry and N. D. Chasteen, *Coord. Chem. Rev.*, 1995, **144**, 347.

4 S. Stefanini, P. Vecchini and E. Chiancone, *Biochem.*, 1987, **26**, 1831.
5 E. Arnold and M. G. Rossmann, *Acta Crystallogr.*, *Sect. A*, 1988, **44**, 270.
6 D. L. D. Caspar and A. Klug, *Physical Principles in the Construction of Regular Viruses*, in *Proceedings of Cold Spring Harbor Symposia on Quantitative Biology*, Long Island Biological Association, New York, 1962, vol. 27.
7 A. Hadfield, J. Hajdu, M. S. Chapman and M. G. Rossmann, *Acta Crystallogr.*, *Sect. D*, *Biol. Crystallogr.*, 1995, **51**, 859.
8 D. M. Lawson, P. J. Artymiuk, S. J. Yewdall, J. M. A. Smith, J. C. Livingstone, A. Treffry, A. Luzzago, S. Levi, P. Arosio, G. Cesarini, C. D. Thomas, W. V. Shaw and P. M. Harrison, *Nature*, 1991, **349**, 541.
9 E. J. W. Whittaker, *Acta Crystallogr.*, 1965, **9**, 855; 862; 865.
10 J. Lu, T. Paliwala, S. C. Lim, C. Yu, T. Niu and A. J. Jacobson, *Inorg. Chem.*, 1997, **36**, 923.
11 O. M. Yaghi, H. Li and T. L. Groy, *Inorg. Chem.*, 1997, **36**, 4292.
12 O. Crespo, M. C. Gimeno, P. G. Jones, A. Laguna and C. Sarroca, *Chem. Commun.*, 1998, 1481.
13 R. K. Kumar, S. Balasubramanian and I. Goldberg, *Chem. Commun.*, 1998, 1435.
14 T. F. Magnera, L. M. Peslherbe, E. Körblová and J. Michl, *J. Organomet. Chem.*, 1997, **548**, 83.
15 B. F. Abrahams, B. F. Hoskins, J. Liu and R. Robson, *J. Am. Chem. Soc.*, 1991, **113**, 3045.
16 M. J. Zaworotko, *Chem. Soc. Rev.*, 1994, 283.
17 D. L. Caulder, R. E. Powers, T. Parac and K. N. Raymond, *Angew. Chem.*, *Int. Ed. Engl.*, 1998, **37**, 1840.
18 C. Brückner, R. E. Powers and K. N. Raymond, *Angew. Chem.*, *Int. Ed. Engl.*, 1998, **37**, 1837.
19 D. L. Caulder and K. N. Raymond, *Angew. Chem.*, *Int. Ed. Engl.*, 1997, **36**, 1439.
20 T. Beissel, R. E. Powers, T. N. Parac and K. N. Raymond, *J. Am. Chem. Soc.*, 1999, in the press.
21 K. N. Raymond, D. L. Caulder, R. E. Powers, T. Beissel, M. Meyer and B. Kersting, *Proc. of the 40th Robert A. Welch Found. on Chem. Res.*, 1996, **40**, 115.
22 L. Carlucci, G. Ciani, P. Macchi and D. M. Proserpio, *Chem. Commun.*, 1998, 1837.
23 J. L. Heinrich, P. A. Berseth and J. R. Long, *Chem. Commun.*, 1998, 1231.
24 K. K. Klausmeyer, T. B. Rauchfuss and S. R. Wilson, *Angew. Chem.*, *Int. Ed. Engl.*, 1998, **37**, 1694.
25 M. Fujita, S.-Y. Yu, T. Kusukawa, H. Funaki, K. Ogura and K. Yamaguchi, *Angew. Chem.*, *Int. Ed. Engl.*, 1998, **37**, 2082.
26 S. Roche, C. Haslam, H. Adams, S. L. Heath and J. A. Thomas, *Chem. Commun.*, 1998, 1681.
27 J. S. Fleming, K. L. V. Mann, C.-A. Carraz, E. Psillakis, J. C. Jeffery, J. A. McCleverty and M. D. Ward, *Angew. Chem.*, *Int. Ed. Engl.*, 1998, **37**, 1279.
28 R. Schneider, M. W. Hosseini, J.-M. Planeix, A. DeCian and J. Fischer, *Chem. Commun.*, 1998, 1625.
29 T. Konno, K. Tokuda and K. Okamoto, *Chem. Commun.*, 1998, 1697.
30 J.-P. Sauvage, *Acc. Chem. Res.*, 1998, **37**, 611.
31 S. B. Lee, S. Hwang, D. S. Chung, H. Yun and J.-I. Hong, *Tetrahedron Lett.*, 1998, **39**, 873.
32 M. Albrecht, *Chem. Soc. Rev.*, 1998, **27**, 281.
33 C. J. Jones, *Chem. Soc. Rev.*, 1998, **27**, 289.
34 E. C. Constable, M. Neuburger, L. A. Whall and M. Zehnder, *New J. Chem.*, 1998, 219.
35 O. D. Fox, N. K. Dalley and R. G. Harrison, *J. Am. Chem. Soc.*, 1998, **120**, 7111.
36 B. Olenyuk, A. Fechtenkötter and P. J. Stang, *J. Chem. Soc.*, *Dalton Trans.*, 1998, 1707.
37 E. J. Enemark and T. D. P. Stack, *Angew. Chem.*, *Int. Ed. Engl.*, 1998, **37**, 932.
38 P. J. Stang, *Chem. Eur. J.*, 1998, **4**, 19.
39 P. J. Stang, N. E. Persky and J. Manna, *J. Am. Chem. Soc.*, 1997, **119**, 4777.
40 P. J. Stang and B. Olenyuk, *Acc. Chem. Res.*, 1997, **30**, 502.
41 C. Piguet, G. Bernardinelli and G. Hopfgartner, *Chem. Rev.*, 1997, **97**, 2005.
42 B. Hasenknopf, J.-M. Lehn, N. Boumediene, A. Dupont-Gervais, A. VanDorsselaer, B. Kneisel and D. Fenske, *J. Am. Chem. Soc.*, 1997, **119**, 10956.
43 B. Hasenknopf, J.-M. Lehn, B. O. Kneisel, G. Baum and D. Fenske, *Angew. Chem.*, *Int. Ed. Engl.*, 1996, **35**, 1838.
44 E. J. Enemark and T. D. P. Stack, *Inorg. Chem.*, 1996, **35**, 2719.
45 E. J. Enemark and T. D. P. Stack, *Angew. Chem.*, *Int. Ed. Engl.*, 1995, **34**, 996.
46 A. F. Williams, *Pure Appl. Chem.*, 1996, **68**, 1285.
47 D. S. Lawrence, T. Jiang and M. Levett, *Chem. Rev.*, 1995, **95**, 2229.
48 M. Fujita, D. Oguro, M. Miyazawa, H. Oka, K. Yamaguchi and K. Ogura, *Nature*, 1995, **378**, 469.
49 R. W. Saalfrank, R. Burak, S. Reihs, N. Löw, F. Hampel, H.-D. Stachel, J. Lentmaier, K. Peters, E.-M. Peters and H. G. vonSchnering, *Angew. Chem.*, *Int. Ed. Engl.*, 1995, **34**, 993.
50 R. W. Saalfrank, R. Burak, A. Breit, D. Stalke, R. Herbst-Irmer, J. Daub, M. Porsch, E. Bill, M. Müther and A. X. Trautwein, *Angew. Chem.*, *Int. Ed. Engl.*, 1994, **33**, 1621.
51 T. Beissel, R. E. Powers and K. N. Raymond, *Angew. Chem.*, *Int. Ed. Engl.*, 1996, **35**, 1084.
52 M. Fujita, J. Yazaki and K. Ogura, *J. Am. Chem. Soc.*, 1990, **112**, 5645.
53 M. Fujita, S. Nagao, M. Iida and K. Ogura, *J. Am. Chem. Soc.*, 1993, **115**, 1574.
54 R. W. Saalfrank, A. Stark, M. Bremer and H. Hummel, *Angew. Chem.*, *Int. Ed. Engl.*, 1990, **29**, 311.
55 F. A. Cotton and G. Wilkinson, *Advanced Inorganic Chemistry*, 5th edn., John Wiley and Sons, New York, 1988.
56 B. A. Borgias, S. J. Barclay and K. N. Raymond, *J. Coord. Chem.*, 1986, **15**, 109.
57 B. Borgias, A. D. Hugi and K. N. Raymond, *Inorg. Chem.*, 1989, **28**, 3538.
58 M. T. Caudle and A. L. Crumbliss, *Inorg. Chem.*, 1994, **33**, 4077.
59 T. M. Garrett, P. W. Miller and K. N. Raymond, *Inorg. Chem.*, 1989, **28**, 128.
60 M. J. Kappel, V. L. Pecoraro and K. N. Raymond, *Inorg. Chem.*, 1985, **24**, 2447.
61 T. B. Karpishin, T. D. P. Stack and K. N. Raymond, *J. Am. Chem. Soc.*, 1993, **115**, 6115.
62 J. Xu and K. N. Raymond, 1999, manuscript in preparation.
63 J. Xu, D. W. Johnson and K. N. Raymond, 1998, unpublished results.
64 CAChe 4.0, Oxford Molecular Group, Inc., USA, 1997.
65 B. Kersting, M. Meyer, R. E. Powers and K. N. Raymond, *J. Am. Chem. Soc.*, 1996, **118**, 7221.
66 M. Meyer, B. Kersting, R. E. Powers and K. N. Raymond, *Inorg. Chem.*, 1997, **36**, 5179.
67 M. Albrecht and S. Kotila, *Angew. Chem.*, *Int. Ed. Engl.*, 1996, 1208.
68 L. J. Charbonniere, G. Bernardinelli, C. Piguet, A. M. Sargeson and A. F. Williams, *J. Chem. Soc.*, *Chem. Commun.*, 1994, 1419.
69 L. J. Charbonniere, M.-F. Gilet, K. Bernauer and A. F. Williams, *Chem. Commun.*, 1996, 39.
70 C. J. Carrano and K. N. Raymond, *J. Chem. Soc.*, *Chem. Commun.*, 1978, 501.
71 C. J. Carrano, S. R. Cooper and K. N. Raymond, *J. Am. Chem. Soc.*, 1979, **101**, 599.
72 R. C. Scarrow, D. L. White and K. N. Raymond, *J. Am. Chem. Soc.*, 1985, **107**, 6540.
73 M. Albrecht and S. Kotila, *Angew. Chem.*, *Int. Ed. Engl.*, 1995, **34**, 2134.
74 M. Albrecht and S. Kotilla, *Chem. Commun.*, 1996, 2309.
75 M. Albrecht, H. Rottele and P. Burger, *Chem. Eur. J.*, 1996, **2**, 1264.
76 M. Albrecht and C. Riether, *Chem. Ber.*, 1996, **129**, 829.
77 J. Xu, T. Parac and K. N. Raymond, *Angew. Chem.*, *Int. Ed. Engl.*, 1999, submitted for publication.
78 Z. Hou, C. J. Sunderland, T. Nishio and K. N. Raymond, *J. Am. Chem. Soc.*, 1996, **118**, 5148.
79 R. W. Saalfrank, B. Horner, D. Stalke and J. Salbeck, *Angew. Chem.*, *Int. Ed. Engl.*, 1993, **32**, 1179.
80 R. E. Powers, *The Rational Design of Supramolecular Assemblies*, Ph.D. Thesis, University of California, Berkeley, CA, 1997.
81 M. Scherer, D. L. Caulder, D. W. Johnson and K. N. Raymond, *Angew. Chem.*, *Int. Ed. Engl.*, 1999, submitted for publication.
82 T. Parac, D. L. Caulder and K. N. Raymond, *J. Am. Chem. Soc.*, 1998, **120**, 8003.
83 P. Jacopozzi and E. Dalcanale, *Angew. Chem.*, *Int. Ed. Engl.*, 1997, **36**, 613.
84 S. Mann, G. Huttner, L. Zsolnai and K. Heinze, *Angew. Chem.*, *Int. Ed. Engl.*, 1996, **35**, 2808.
85 J. Bryant, M. T. Blanda, M. Vincenti and D. J. Cram, *J. Am. Chem. Soc.*, 1991, **113**, 2167.
86 P. Timmerman, W. Verboom, F. C. J. M. vanVeggel, J. P. M. vanDuynhoven and D. N. Reinhoudt, *Angew. Chem.*, *Int. Ed. Engl.*, 1994, **33**, 2345.
87 D. L. Kepert, *Inorganic Stereochemistry*, Springer Verlag, Heidelberg, 1982.
88 A. J. Amoroso, J. C. Jeffery, P. L. Jones, J. A. McCleverty, P. Thornton and M. D. Ward, *Angew. Chem.*, *Int. Ed. Engl.*, 1995, **34**, 1443.

89 X. Sun, D. W. Johnson, D. L. Caulder, R. E. Powers, K. N. Raymond and E. H. Wong, *Angew. Chem.*, *Int. Ed. Engl.*, 1999, in the press.
90 C. G. Pierpoint and R. M. Buchanan, *Coord. Chem. Rev.*, 1981, **38**, 45.
91 C. G. Pierpoint and C. W. Lange, *Inorg. Chem.*, 1994, **41**, 331.
92 C. A. McAuliffe, in *Comprehensive Coordination Chemistry*, vol. 2, ed. G. Wilkinson, F. G. A. Stone and F. W. Abel, Pergamon, Oxford, 1987, ch. 14.
93 W. Levason, in *The Chemistry of Organophosphorus Compounds*, vol. 1, ed. F. R. Hartley, Wiley, New York, 1990, ch. 16.
94 M. Fujita, O. Sasaki, T. Mitsuhashi, T. Fujita, J. Yazaki, K. Yamaguchi and K. Ogura, *Chem. Commun.*, 1996, 1535.
95 F. H. Allen and O. Kennard, *Chem. Des. Automat. News*, 1993, **8**, 31.
96 P. J. Stang and D. H. Cao, *J. Am. Chem. Soc.*, 1994, **116**, 4981.
97 B. Kersting, J. R. Telford, M. Meyer and K. N. Raymond, *J. Am. Chem. Soc.*, 1996, **118**, 5712.
98 J. R. Hutchison, J. G. Gordon and R. H. Holm, *Inorg. Chem.*, 1971, **10**, 1004.
99 R. C. Fay and T. S. Piper, *Inorg. Chem.*, 1964, **3**, 348.
100 S. S. Eaton, G. R. Eaton, R. H. Holm and E. L. Muetterties, *J. Am. Chem. Soc.*, 1973, **95**, 116.
101 R. Krämer, J.-M. Lehn and A. Marquis-Rigault, *Proc. Natl. Acad. Sci.*, *USA*, 1993, **90**, 5394.
102 M. A. Masood, E. J. Enemark and T. D. P. Stack, *Angew. Chem.*, *Int. Ed. Engl.*, 1998, **37**, 928.
103 C. S. G. Phillips and R. J. P. Williams, *Inorganic Chemistry*, 1st edn., vol. 1, Oxford University Press, New York, 1965.
104 I. M. Klotz, *Ligand-Receptor Energetics*, 1st edn., John Wiley & Sons, Inc., New York, 1997.
105 T. N. Parac, D. L. Caulder and K. N. Raymond, 1999, manuscript in preparation.
106 R. Krämer, J.-M. Lehn, A. DeCian and J. Fischer, *Angew. Chem.*, *Int. Ed. Engl.*, 1993, **32**, 703.
107 C. Provent, S. Hewage, G. Brand, G. Bernardinelli, L. J. Charbonniére and A. F. Williams, *Angew. Chem.*, *Int. Ed. Engl.*, 1997, **36**, 1287.
108 F. M. Romero, R. Ziessel, A. Dupont-Gervais and A. VanDorsselaer, *Chem. Commun.*, 1996, 551.
109 P. N. W. Baxter and J.-M. Lehn, *Chem. Commun.*, 1997, 1323.

Paper 8/08370C